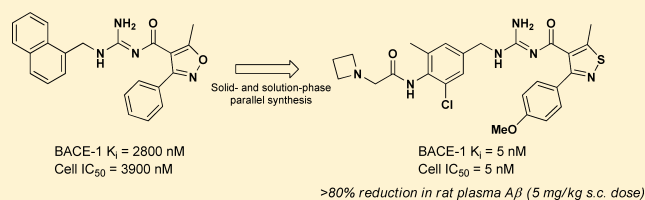


Acyl Guanidine Inhibitors of β -Secretase (BACE-1): Optimization of a Micromolar Hit to a Nanomolar Lead via Iterative Solid- and Solution-Phase Library SynthesisSamuel W. Gerritz,^{*,†} Weixu Zhai,[†] Shuhao Shi,[†] Shirong Zhu,[†] Jeremy H. Toyn,[†] Jere E. Meredith, Jr.,[†] Lawrence G. Iben,[†] Catherine R. Burton,[†] Charles F. Albright,[†] Andrew C. Good,[†] Andrew J. Tebben,[‡] Jodi K. Muckelbauer,[‡] Daniel M. Camac,[‡] William Metzler,[‡] Lynda S. Cook,[†] Ramesh Padmanabha,[†] Kimberley A. Lentz,[†] Michael J. Sofia,[†] Michael A. Poss,[‡] John E. Macor,[†] and Lorin A. Thompson, III[†][†]Bristol-Myers Squibb Research, 5 Research Parkway, Wallingford, Connecticut 06492, United States[‡]Bristol-Myers Squibb Research, P.O. Box 4000, Princeton, New Jersey 08543-4000, United States

Supporting Information

ABSTRACT: This report describes the discovery and optimization of a BACE-1 inhibitor series containing an unusual acyl guanidine chemotype that was originally synthesized as part of a 6041-membered solid-phase library. The synthesis of multiple follow-up solid- and solution-phase libraries facilitated the optimization of the original micromolar hit into a single-digit nanomolar BACE-1 inhibitor in both radioligand binding and cell-based functional assay formats. The X-ray structure of representative inhibitors bound to BACE-1 revealed a number of key ligand:protein interactions, including a hydrogen bond between the side chain amide of flap residue Gln73 and the acyl guanidine carbonyl group, and a cation- π interaction between Arg235 and the isothiazole 4-methoxyphenyl substituent. Following subcutaneous administration in rats, an acyl guanidine inhibitor with single-digit nanomolar activity in cells afforded good plasma exposures and a dose-dependent reduction in plasma A β levels, but poor brain exposure was observed (likely due to Pgp-mediated efflux), and significant reductions in brain A β levels were not obtained.



INTRODUCTION

Alzheimer's disease (AD) is a progressive neurodegenerative disorder whose effects are initially manifested in the loss of short-term memory, followed by increasingly worsening senile dementia and leading ultimately to death.¹ In 2009, it was estimated that AD afflicted more than 35 million people worldwide.² Current treatments include the acetylcholinesterase inhibitors and the NMDA blocker memantine; however, these agents treat disease symptoms and do not halt or delay disease progression. AD is defined by two characteristic brain lesions, intraneuronal neurofibrillary tangles comprising a hyperphosphorylated form of the microtubule-binding protein tau and extracellular amyloid plaques comprising a complex mixture of β -amyloid (A β) peptides spanning 36 to 43 amino acids. Data derived from studies of genetic mutations in early onset AD suggest that overproduction of A β 1–42 is a significant contributor to AD.³ Substantial progress in understanding the underlying etiology of AD has been made over the past decade, and current work suggests that soluble forms of A β 1–42 are central to the disease process.³ Therapeutic agents that reduce A β production in the brain thus represent a logical approach to discovering a disease-modifying therapy.⁴ A β is produced via sequential proteolytic cleavage of amyloid precursor protein (APP) by two enzymes:¹ (1) β -APP-

cleaving enzyme 1 (BACE-1, also called β -secretase), an aspartyl protease that performs a selective proteolysis of APP to afford the N-terminus of A β , and (2) γ -secretase, a protein complex with presenilin at its catalytic core that cleaves APP to generate the C-terminus. Inhibiting either of these enzymes blocks the production of A β , prevents the formation of β -amyloid plaques, and reverses amyloid-induced cognitive deficits in laboratory animals.⁵ In this paper, we report the discovery and optimization of a novel series of acyl guanidine-based BACE-1 inhibitors.

RESULTS AND DISCUSSION

Owing to their peptidomimetic origins, early BACE-1 inhibitors⁶ contained multiple amide bonds and polar functional groups, which served to limit their brain exposure. In an effort to discover novel nonpeptidic BACE-1 inhibitors, we performed a structure-biased fragment screening campaign in which fragments that scored high in a BACE-1 binding model were tested in an NMR direct binding assay and a high concentration (30 μ M) HTS assay. These screening efforts

Special Issue: Alzheimer's Disease

Received: July 2, 2012

Published: September 4, 2012

culminated in the discovery of acyl guanidine **1** (Figure 1). When tested in our radioligand binding assay,⁷ **1** afforded a

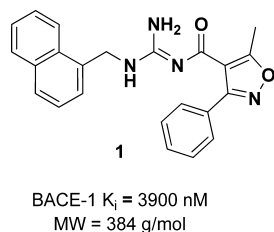


Figure 1. BACE-1 HTS hit acyl guanidine **1**.

BACE-1 K_i = 3900 nM, several orders of magnitude less potent than that of reported peptide-based inhibitors. The ligand efficiency^{8,9} (LE) of compound **1** was 0.25 kcal/mol-heavy atom, utilizing the following equation: $LE = -RT \ln(K_i)/\text{heavy atom count}$, and this value was relatively low for a nascent screening hit. However, the unusual structure and ease of synthesis of **1** prompted further exploration of the chemotype in search of improved BACE-1 activity. Compound **1** was initially synthesized¹⁰ on solid phase as part of a 6041-membered, ion channel-targeted library comprising two points of diversity: (1) an amine reagent set (e.g., the 1-aminomethyl-naphthyl side chain of **1**) and (2) a carboxylic acid reagent set (e.g., the 5-methyl-3-phenylisoxazole moiety of **1**). Although **1** was originally submitted as a crude library product with an HPLC purity of 70% (based on UV absorbance, $\lambda = 254$ nm), the resynthesis and purification of **1** successfully recapitulated the observed BACE-1 activity.

The library pedigree of **1** provided a robust solid-phase synthesis of acyl guanidines as shown in Scheme 1. The synthesis commenced with treatment of commercially available *p*-nitrophenylcarbonate-modified polystyrene Wang (PS-Wang) resin¹¹ (**2**) with *S*-methylisothiourea under basic conditions to provide the corresponding solid-supported carbamate **3**. By utilizing carefully optimized conditions (PyAOP, DIEA), the primary nitrogen of **3** was acylated with carboxylic acid **4** to provide the polymer-bound *S*-methylthiourea **5** and, in the process, activating the thiomethyl group for subsequent displacement by amine **6** to afford the solid-supported carbamate-protected acyl guanidine **7**. Treatment of **7** with TFA provided acyl guanidine **8**. In the case of the aforementioned ion channel library, compound **8** analogues

were submitted without further purification, but for the BACE-1 hit-to-lead efforts described herein, all analogues of compound **8** were purified via reverse-phase HPLC prior to submission for biological testing.

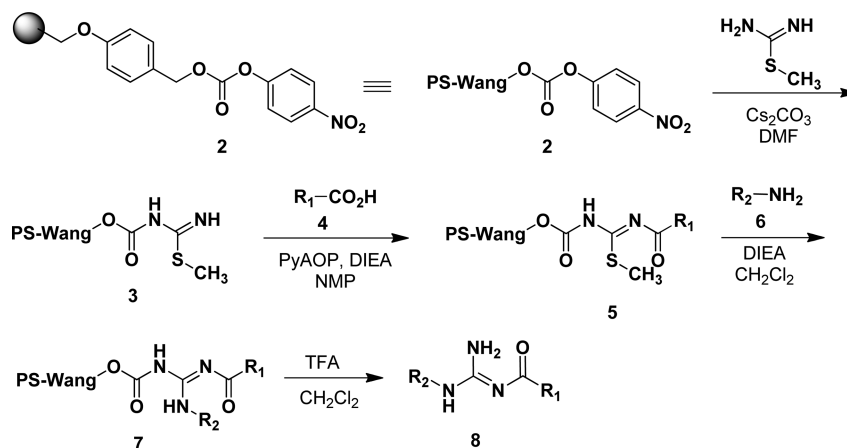
Over 5000 acyl guanidine analogues were assayed in the BACE-1 HTS, and every active sample contained both the 5-methyl-3-phenyl isoxazole (R_1) found in **1** and a small group of benzylamine (R_2) substructures. The high degree of structural similarity among the HTS hits prompted the synthesis of a matrix library in which the benzylamine and isoxazole^{10,11} side chains were varied simultaneously. Table 1 summarizes the

Table 1. Acyl Guanidine Matrix Library Summary

Compound	R_1	R_2	BACE-1 K_i (nM) ^a
1		H	2800
8a		F	1800
8b		OMe	1700
8c		H	>10,000
8d		F	>10,000
8e		OMe	4000
8f		H	8800
8g		F	2400
8h		OMe	910
8i		H	3900
8j		F	2200
8k		OMe	670

^aMean radioligand displacement activity ($n \geq 2$) according to ref 7. Each K_i value is within 2.2-fold of the mean.

Scheme 1

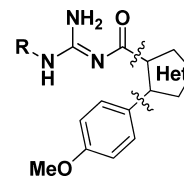


BACE-1 activity for a 4 amine (R_1) \times 3 acid (R_2) matrix and highlights how a matrix approach can afford greater SAR insight than optimizing a single position at a time. For example, when $R_1 = 1$ -naphthylmethyl, the R_2 substituent does not appear to have a significant effect on BACE-1 activity (cf. **1** vs **8a** vs **8b**). However, when $R_1 = 3,4$ -dichlorobenzyl, the R_2 substituent strongly influences the BACE-1 activity as seen by the progression from **8f** ($R_2 = H$) to **8g** ($R_2 = F$) to **8h** ($R_2 = OMe$); with a $K_i = 910$ nM, compound **8h** represents a nearly 10-fold improvement in BACE-1 activity over **8f** ($K_i = 8800$ nM). The same trend is observed when $R_1 = 3,5$ -dichlorobenzyl (analogues **8i**–**8k**), and this side chain afforded the most potent analogue synthesized to date (**8k**) with a BACE-1 $K_i = 670$ nM. Given that the number of heavy atoms did not change from **1** to **8k**, the LE improved from 0.25 kcal/mol-heavy atom to 0.29 kcal/mol-heavy atom. The 3,5-dichlorobenzyl side chain replaced the 1-naphthylmethyl side chain for all subsequent SAR studies, and it is likely that this side chain would not have been identified without synthesizing a matrix library, as the significance of the $R_2 = OMe$ substituent was not apparent in the 1-naphthylmethyl series (cf. **1** and **8b**), and the activity enhancement provided by the 3,5-dichlorobenzyl side chain was not observed when $R_2 = H$ (cf. **1** and **8i**); it was only when R_1 and R_2 were varied simultaneously that a substantial improvement in activity was realized.

The discovery of compound **8k** prompted us to hold the 3,5-dichlorobenzyl side chain constant and explore the isoxazole side chain more extensively. This effort did not afford a significant improvement in BACE-1 activity, but it did provide two key SAR findings (Supporting Information, Table SI-1): (1) the 5-position methyl group was required for activity (i.e., the 5-H and 5-Et analogues were inactive), and (2) although the SAR for the 3-phenyl side chain was fairly flat, we observed a consistent preference for electron-donating substituents (i.e., 4-MeO). This SAR was applied to the exploration of isoxazole replacements, as shown in Table 2. The “reverse” isoxazole **8l** afforded similar BACE-1 activity as the parent (**8k**), but pyrazole **8m** and isothiazole **8o** both provided a modest but reproducible increase in BACE-1 activity. The *N*-methyl analogue (**8n**) of pyrazole **8m** was 20-fold less potent in the BACE-1 binding assay, suggesting that the nitrogen of **8m** (and **8k**) engaged in a direct interaction with the BACE-1 protein. Even though pyrazole **8m** and isothiazole **8o** were equipotent, the pyrazole introduced another H-bond donor and this prompted us to focus on isoxazoles and isothiazoles for subsequent analogue efforts. The discovery of isothiazole **8o** prompted a re-examination of benzylamine substitution (Table 2, entries **8p**–**8s**). Although the benzylamine SAR remained narrow, two close analogues of the 3,5-dichlorobenzyl group were equipotent with **8k**: the 3-bromo-5-chlorobenzyl analogue **8r** was an important precursor for a subsequent Suzuki coupling library and the 3,5-dimethylbenzyl analogue **8s** suggested that chloro and methyl substituents could be used interchangeably.

Starting with compound **1**, the iterative synthesis of solid-phase libraries led to the identification of **8o** and a 10-fold improvement in BACE-1 potency. However, with a BACE-1 $K_i = 290$ nM, the potency of **8o** remained at least an order of magnitude from presumed therapeutic utility, and ensuing optimization efforts focused on exploiting protein–ligand interactions established for other classes of BACE-1 ligands. To elucidate the binding mode of acyl guanidines to BACE-1, X-ray crystallography efforts were initiated with compound **8k**.

Table 2. Heterocyclic Isoxazole Replacements



Compound	R	Het	BACE-1 K_i (nM) ^a	
8k			670	
8l			860	
8m			210	
8n			4000	
8o			290	
8p				500
8q				870
8r				270
8s				280

^aMean radioligand displacement activity ($n \geq 2$) according to ref 7. Each K_i value is within 2.2-fold of the mean.

Co-crystals of a Phe-statine peptide^{13,14} bound to BACE-1 were soaked with **8k**, X-ray diffraction data were collected, and the structure was determined. Initial electron density maps were of marginal quality due to data resolution (2.8 Å) and incomplete displacement of the Phe-statine peptide, resulting in partial

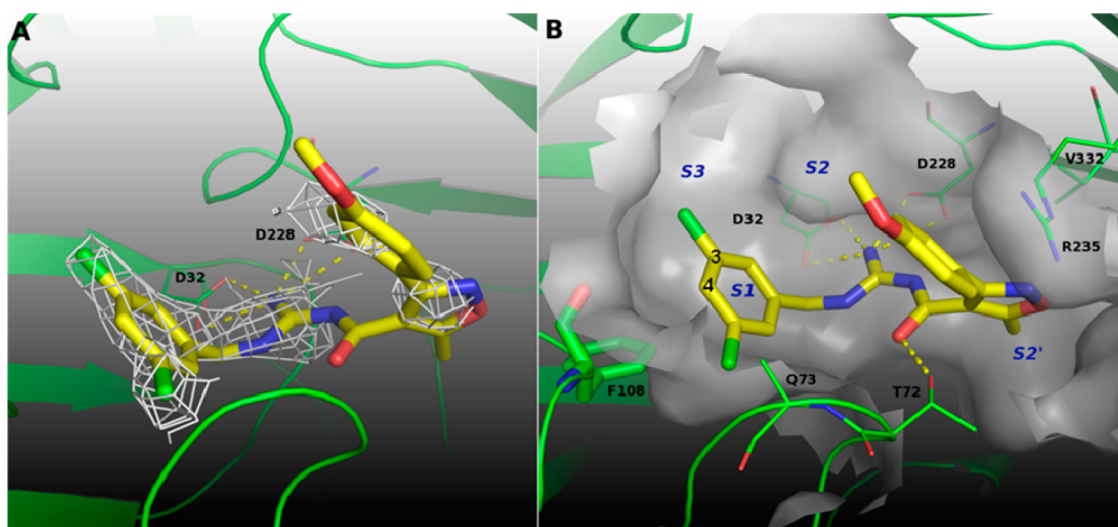
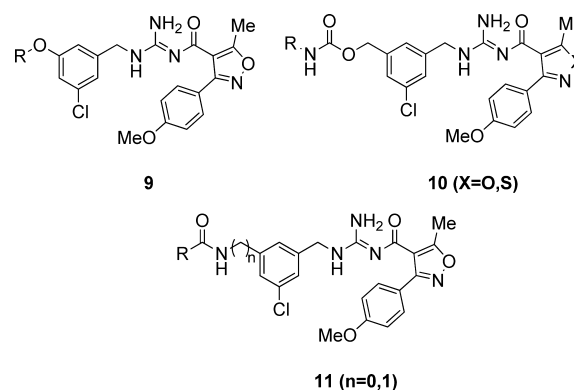


Figure 2. Computational model of **8k** bound to BACE-1 derived from the X-ray crystal structure. (A) Initial density of compound **8k** contoured at 1.0σ (white mesh). Contiguous electron density is present for the 3,5-dichlorobenzyl and guanidine moieties but is incomplete for the acyl-isoxazole and 4-methoxyphenyl groups. The computational model derived from the crystal structure is shown for reference (yellow carbons). Hydrogen bonds to the conserved catalytic aspartates, Asp32 and Asp228, are shown as hashed yellow lines. (B) Computational model of **8k** (yellow carbons) bound to BACE-1. Residues predicted to form key contacts with **8k** are shown as thin green sticks. Subsites within the BACE1 active site are indicated with blue text. F108 is shown as thick green sticks. The figures were produced using Pymol.¹⁶

density for compound **8k**. Even so, the electron density map provided sufficient information to unambiguously place the acyl guanidine and the 3,5-dichlorobenzyl groups of **8k** in the active site of BACE-1 (Figure 2A). The 3,5-dichlorobenzyl side chain occupies the S1 pocket, and the acyl guanidine forms hydrogen bonds with Asp32 and Asp228. The electron density for the 3-(4-methoxyphenyl)-5-methylisoxazole side chain of **8k** was very weak, making unambiguous placement of this group impossible. This resulted in a partial model of **8k** bound to BACE-1. Computational modeling was then used to evaluate the two potential positions of the 4-methoxyphenyl side chain, one which placed it in the S2' pocket and a second orienting it in the S2 pocket. The model of the former configuration resulted in steric clashes with the side chain of Val332, ruling it out as a reasonable bound conformation. No steric clashes were observed in the S2 model, and so it was utilized as the structural basis for further design as shown in Figure 2B. The information gleaned from the X-ray crystal structure and the computational models of BACE-1 with **8k** suggested two potential strategies for improving BACE-1 binding affinity. First, it was apparent that the S3 site was unoccupied. Knowing that introduction of substituents into the S3 pocket is a well precedented strategy for improving BACE-1 binding affinity,^{13–15} chemistry efforts were initiated at the 3-position of the benzylamine side chain to reach into the S3 pocket. The model also revealed that the backbone carbonyl of Phe108, at the edge of the S1 pocket, was exposed and less than 4 Å from the 4-position of the benzylamine of **8k**. The proximity of this carbonyl to the benzylamine suggested that the addition of hydrogen bond donors to the 4-position could form favorable interactions, and chemistry efforts were directed toward a second set of analogues to investigate this hypothesis.

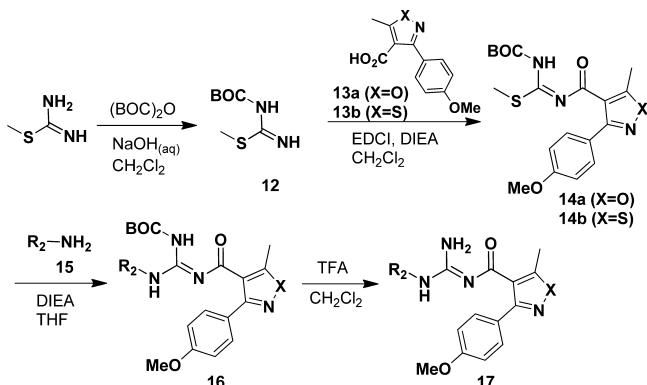
Our initial efforts to increase BACE-1 potency via occupation of the S3 pocket focused on the parallel synthesis of ethers (i.e., **9**), carbamates (i.e., **10**), and amides (i.e., **11**) obtained via Mitsunobu alkylation of solid-supported phenols, carbamoylation of solid-supported benzyl alcohols, and acylation of solid-supported amines, respectively (Supporting Information, Figure

SI-1). As described in Tables SI-2 and SI-3 in the Supporting Information, these analogues did not afford improved BACE-1 activity, and we turned our attention to C-linked analogues as described below.



The solid-phase synthesis of acyl guanidines (Scheme 1) offered a number of advantages over a solution-phase synthesis, including the ability to utilize a split-mix synthetic protocol for the rapid synthesis of small matrices of analogues in which both the R_1 and R_2 substituents were varied. In addition, the crude acyl guanidine product was generally very pure and this greatly facilitated the final purification step via preparatory HPLC. However, solid-phase synthesis is generally not the most efficient method for the synthesis of multigram quantities of material, and so we developed a solution-phase route to acyl guanidines as shown in Scheme 2. By analogy to the synthesis of a CBZ-protected guanidinyllating reagent,¹⁷ treatment of *S*-methylisothiourea with BOC anhydride provided BOC-*S*-methylisothiourea **12** as a crystalline, stable solid. Acylation of **12** under standard conditions with our preferred isoxazole (**13a**) or isothiazole (**13b**) provided *S*-methylisothiourea **14a** (or **14b**), which upon sequential treatment with amine **15** and TFA afforded acyl guanidine **17**. We routinely synthesized multigram quantities of intermediates **14a** and **14b** and utilized

Scheme 2



this chemistry to synthesize gram quantities of key intermediates, including the 3-bromo-5-chlorobenzyl analogue **8r** as the penultimate intermediate in the synthesis of C-linked 3-benzyl analogues via Suzuki coupling chemistry.

As shown in eq 1, **8r** facilitated the introduction of aryl and alkenyl side chains via straightforward Suzuki chemistry. As

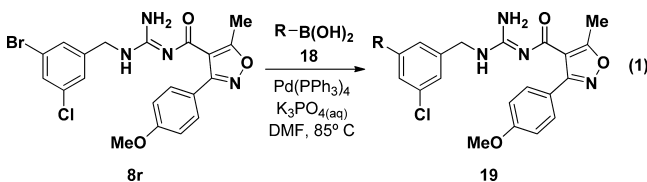


Table 3. BACE-1 Activity of 3-Aryl and 3-Alkenyl Analogues

Compound	R	BACE-1 K_i (nM) ^a
8r	Br	510
19a		1200
19b		1800
19c		430
19d		140
19e		850
19f		150

^aMean radioligand displacement activity ($n \geq 2$) according to ref 7. Each K_i value is within 2.2-fold of the mean.

summarized in Table 3, aryl side chains (i.e., **19a** and **19b**) were significantly less active than alkenyl substituents, possibly because the resulting biphenyl group was too rigid to effectively “reach” into the S3 pocket. In contrast, small alkene substituents (i.e., **19c**) were equipotent with **8r**, but we were intrigued that introduction of an oxygen, either as an alcohol (**19d**) or ether (**19f**), 3 or 4 atoms distal from the phenyl ring afforded a significant improvement in activity, particularly in comparison to the “all carbon” analogue **19e**. Even though **19d** and **19f** were among the most potent acyl guanidines identified at the time, two concerns prompted us to abandon this SAR vector: (1) the preference for oxygen-containing substituents suggested displacement of an adjacent H₂O molecule rather than occupation of the highly lipophilic S3 pocket, (2) in other chemotypes, introducing substituents which occupied the S3 pocket afforded improvements in BACE-1 activity on the order of 10–100-fold^{13–15} rather than the modest 4-fold improvement observed between **8r** ($K_i = 510$ nM) and **19d** ($K_i = 140$ nM).

Having failed to identify substituents that occupy the S3 pocket, we turned our attention to substituents at the 4-position of the benzylamine side chain, as the binding model shown in Figure 1 suggested that BACE-1 backbone amide bonds lay in close proximity. The chemistry to access these 4-position analogues proved challenging, as the 3,5-dichloro substitution pattern imparted significant steric and electronic barriers to substitution at the 4-position. This necessitated the introduction of the entire 4-position side chain prior to the reaction of benzylamine **15** with **14a** (or **14b**). As shown in Table 4, the 4-OH analogue **17a** did not afford any

Table 4. BACE-1 Activity of 4-Substituted-3,5-Dichlorobenzylamine Analogues

compd	X	R	BACE-1 K_i (nM) ^a	HEK-Sw IC_{50} (nM) ^{b,c}
8k	O	H	670	1600
8o	S	H	290	>5000
17a	O	OH	480	nd
17b	O	O- <i>n</i> Pr	>5000	nd
17c	O	NH ₂	120	nd
17d	S	NH ₂	40	630
17e	O	NHC(=O)CH ₃	10	790
17f	S	NHC(=O)CH ₃	5	310

^aMean radioligand displacement activity ($n \geq 2$) according to ref 7. Each K_i value is within 2.2-fold of the mean. ^bMean A β -lowering activity in HEK 293 cells ($n \geq 2$) according to ref 18. Each IC_{50} value is within 1.6-fold of the mean. ^cnd = not determined.

improvement in BACE-1 activity, and the corresponding *n*-Pr ether **17b** was inactive. However, the 4-NH₂ side chain provided a dramatic increase in activity with both the isoxazole (**17c**, $K_i = 120$ nM) and isothiazole (**17d**, $K_i = 40$ nM) analogues. With an LE of 0.34 kcal/mol·heavy atom, **17d** provided a significant improvement in ligand efficiency. Acetylation of the 4-NH₂ group afforded two very potent acyl guanidines: isoxazole **17e** ($K_i = 10$ nM) and isothiazole **17f** ($K_i = 5$ nM), both of which were approximately 60-fold more

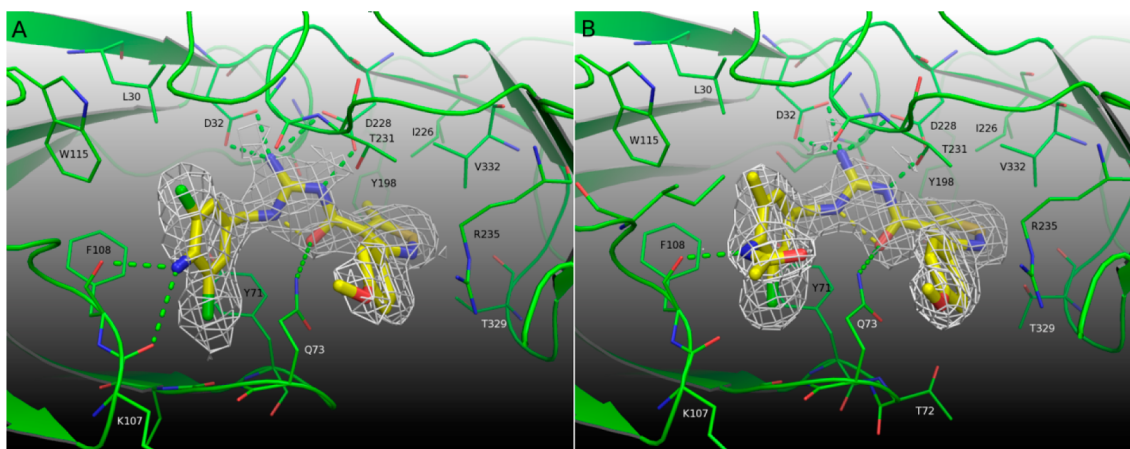


Figure 3. Crystal structures of compounds 17d (A) and 17g (B) bound to BACE1. Ligands are rendered in yellow sticks. Refined ligand electron density contoured at 1.0σ is shown as white mesh. Residues within 4.0 Å of the ligand are shown as thin green sticks. Protein–ligand hydrogen bonds are indicated as green dashed lines and ligand intramolecular hydrogen bonds as yellow dashed lines. The figures were produced using Pymol.¹⁶

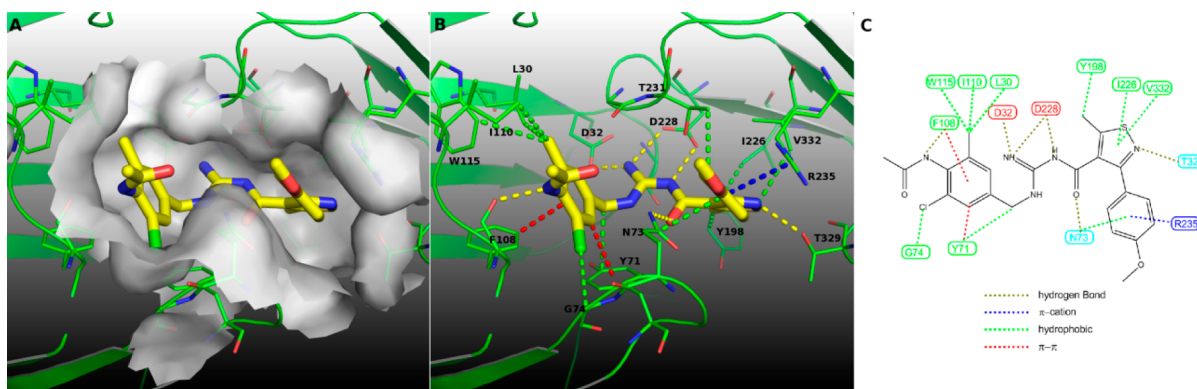


Figure 4. Interactions between BACE1 (green) and compound 17g (yellow) rendered as a surface view (A), in 3D (B), and 2D (C). Ligand:protein bonding interactions are depicted as dashed lines: hydrogen bonds, yellow; π - π , red; π -cation, blue; hydrophobic, green. The figures were produced using Pymol.¹⁶

Table 5. Binding and Cellular BACE-1 Activity of 4-Acylamino Analogues

compd	X	R ₁	R ₂	BACE-1 K _i (nM) ^a	HEK-Sw IC ₅₀ (nM) ^b	IC ₅₀ /K _i ratio
17f	S	Cl	CH ₃ C(=O)	5	310	62
17g	S	Me	CH ₃ C(=O)	20	240	12
17h	S	Cl	CH ₃ S(=O) ₂	280	nd ^c	
17i	O	Me	CH ₃ CH ₂ C(=O)	40	780	19
17j	S	Me	PhC(=O)	30	430	13
17k	O	Cl	CH ₃ SCH ₂ C(=O)	50	2000	40
17l	O	Me	CH ₃ SCH ₂ CH ₂ C(=O)	30	640	21
17m	O	Cl	CH ₃ S(=O) ₂ CH ₂ C(=O)	30	1900	63
17n	O	Cl	cyclopropylC(=O)	50	1600	32
17o	O	Me	cyclopropylC(=O)	20	330	16
17p	O	Me	2-furylC(=O)	60	1400	23
17q	O	Cl	(CH ₃) ₂ NCH ₂ C(=O)	50	210	4
17r	O	Me	(CH ₃) ₂ NCH ₂ C(=O)	50	90	2

^aMean radioligand displacement activity ($n \geq 2$) according to ref 7. Each K_i value is within 2.2-fold of the mean. ^bMean A β lowering activity in HEK 293 cells ($n \geq 2$) according to ref 18. ^cnd = not determined. Each IC₅₀ value is within 1.6-fold of the mean.

Scheme 3

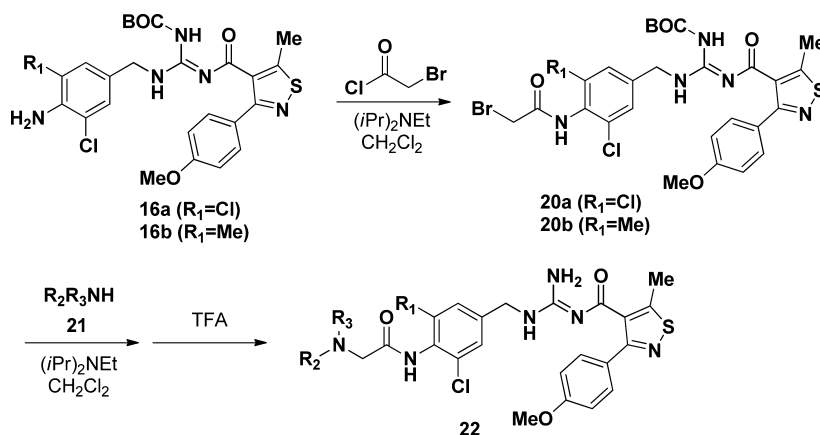


Table 6. Binding and Cellular BACE-1 Activity of Aminoacetamide Analogues

Compound	R_1	NR_2R_3	BACE-1 K_i (nM) ^a	HEK-Sw IC_{50} (nM) ^b	IC_{50}/K_i Ratio
22a	Cl	Me ₂ N	20	70	4
22b	Me		20	20	1
22c	Cl	PhCH ₂ NH	6	140	23
22d	Me		10	70	7
22e	Cl	EtNH	10	20	2
22f	Me		20	10	0.5
22g	Cl		4	8	2
22h	Me		5	5	1

^aMean radioligand displacement activity ($n \geq 2$) according to ref 7. Each K_i value is within 2.2-fold of the mean. ^bMean $A\beta$ lowering activity in HEK 293 cells ($n \geq 2$) according to ref 18. Each IC_{50} value is within 1.6-fold of the mean.

potent than the corresponding 4-H analogues (**8k** and **8o**, respectively). Compound **17f** maintained an LE of 0.34 kcal/mol-heavy atom. Along with the dramatic improvement in BACE-1 binding activity, these potent analogues were also the first acyl guanidine analogues to afford submicromolar activity in our cell-based (HEK-Sw) assay¹⁸ in which HEK cells were engineered to overexpress amyloid precursor protein (APP) containing the Swedish mutation and the effect of BACE-1 inhibitors on the production of $A\beta$ was measured via ELISA. The consistent disparity between binding and cellular activity will be discussed in greater detail.

At this point, we were gratified to obtain the X-ray crystal structure of **17d** bound to BACE-1 (Figure 3A). Initial electron density maps were of good quality and revealed unambiguous

density for the entire compound. This structure was largely consistent with the partial X-ray structure and resulting computational model of **8k** bound to BACE-1 (Figure 2); in particular, it confirmed the predicted orientation of the 3-(4-methoxyphenyl)-5-methylisoxazole into the S2 pocket (Figure 3A). As anticipated from SAR and modeling, the amino group at the 4-position of the benzylamine side chain of **17d** formed a hydrogen bond to the backbone carbonyl of Phe108, and we observed an additional hydrogen bond to the backbone carbonyl from Lys107. Collectively, these hydrogen bonds provide a structural basis for the observed increase in potency. The structure also revealed an unexpected conformation of the side chain of flap residue Gln73, allowing the Gln73 side chain to form a hydrogen bond to the isoxazole carbonyl oxygen of

17d. The unanticipated conformation of the Gln73 side chain is additionally stabilized by van der Waals interactions with the 4-methoxyphenyl group of the isoxazole. A crystal structure of the *N*-acetyl analogue **17g** was also obtained (Figure 3B). In this structure, a hydrogen bond between the backbone carbonyl of Phe108 and the acetamide NH is observed with the acetamide moiety itself being oriented away from the S1 pocket, toward solvent. The structure also reveals a total of 18 protein–ligand interactions encompassing nearly every heavy atom of **17g** and highlighting the high ligand efficiency for the series (Figure 4).

The discovery of the 4-acetamido-3,5-dichlorobenzyl analogues **17e** and **17f** prompted a thorough exploration of other 4-acylamino groups (and acylamino mimetics) as summarized in Table 5. The SAR for 4-acylamino analogues was largely flat; replacing the carbonyl group of **17f** with a sulfonyl group (**17h**) had a detrimental effect on the BACE-1 K_i value, but otherwise all of the acyl analogues contained in Table 5 were equipotent. However, while developing the chemistry to access these analogues, we discovered an unusual phenomenon: when a 3-methyl group was substituted for the 3-chloro group in compound **17f**, the ratio between the BACE-1 IC_{50} (measured in the cellular/HEK-Sw assay) and the BACE-1 K_i (measured in the radioligand binding assay) was consistently lower for the methyl analogue (**17g**). This trend was also observed with analogues **17n** and **17o**: the BACE-1 K_i values were not affected (within experimental error) by the change from $R_1 = Cl$ to $R_1 = Me$, but the methyl-containing compound **17o** was 5-fold more potent in the HEK-Sw assay. We have no explanation for this “methyl effect” on cellular potency, and we were further surprised by the 4-(2-(*N,N*-dimethylamino)-acetamido) analogues **17q** and **17r**; in this case, the introduction of a basic side chain dramatically improved the cellular activity and provided IC_{50} to K_i ratios approaching unity. A similar “ pK_a effect” on cellular potency has been reported^{19,20} for two structurally unrelated BACE-1 chemotypes, but our case is unique in several respects. In the first report,¹⁹ the authors discovered that increasing the pK_a of an amino group that directly interacts with the active site aspartates afforded an activity increase in *both* binding and cellular assays. In contrast, the basic side chain of our series is distal to the active site and the activity increase is observed *only* in the cellular assay; the binding activity is unaffected. In the second report,²⁰ a 3-fold improvement in cellular activity (with no effect on binding activity) was obtained when a pyridyl N was substituted for a phenyl CH, although the ratio between cellular and binding activities remained high at 19-fold. This is consistent with our observation, although the magnitude of the shift in our series is more pronounced: introduction of a basic amine afforded an 8-fold improvement in cellular activity (cf. **17i** and **17r**), and a 2- to 4-fold IC_{50} to K_i ratio. The origin of this “basic amine effect” is likely the result of altered drug distribution within cells, and we hypothesize that the basic amine modifies the physical properties of this series to afford a higher effective concentration of drug within the cellular compartment where BACE-1 processes $A\beta$.

Additional amine-containing analogues were synthesized from α -bromoacetamide intermediates **20a** and **20b** as shown in Scheme 3, and the BACE-1 binding and cellular data are summarized in Table 6. Comparing the IC_{50}/K_i ratios for each pair of analogues (i.e., **22a** and **22b**, **22c** and **22d**) provided additional evidence for the aforementioned “methyl effect” on cellular potency. Combined with the “basic amine effect” on cellular potency, a number of samples with low nM activity in

both the BACE-1 binding and HEK-Sw cellular assays were identified, and azetidine-containing analogue **22h** emerged as the most potent acyl guanidine identified to date, with single-digit nanomolar activity in both assays. Compound **22h** exhibited no Herg activity in a thallium flux assay²¹ and was inactive against a panel of aspartyl proteases⁷ (i.e., cathepsin D, cathepsin E, and pepsin; Supporting Information Table SI-4).

As described previously, acetamide analogues bearing a basic side chain (i.e., **17q–17r**, **22a–22h**) afforded a significant increase in activity in the cellular assay relative to nonbasic acetamides (i.e., **17f–17p**), with little or no effect on activity in the binding assay. We were thus not surprised to find that the X-ray co-crystal structure of **17r** and BACE-1 (unpublished data) did not reveal any additional ligand–protein interactions, and the pendant *N,N*-dimethylamino group appears to be solvent-exposed. However, we did note the close proximity of the *N,N*-dimethylamino group and the 4-methoxyphenyl group of the isoxazole; in the crystal structure, the C–C distance between these methyl groups is 4.9 Å. This observation prompted the development of a straightforward ring-closing metathesis route to macrocyclic isoxazolyl acyl guanidines, and the synthesis and biological properties of these macrocycles will be described in a future publication.

The cellular potency of compound **22h** prompted us to evaluate its effect on $A\beta$ 1–40 levels in the plasma, brain, and cerebral spinal fluid (CSF) of rats.^{13,18} Three subcutaneous (sc) doses were selected: 5, 15, and 40 mg/kg, and $A\beta$ 1–40 and drug levels were measured 5 h after administration of **22h**. The 40 mg/kg group was pretreated with a 50 mg/kg oral dose of aminobenzotriazole (ABT), a pan-cytochrome P450 (CYP P450) inhibitor, in order to improve drug levels by blocking CYP-mediated metabolism. As shown in Figure 5, dramatic and dose-dependent reductions in plasma $A\beta$ 1–40 were observed. However, despite the robust peripheral effect, significant reductions of brain or CSF $A\beta$ 1–40 were not observed at any dose.

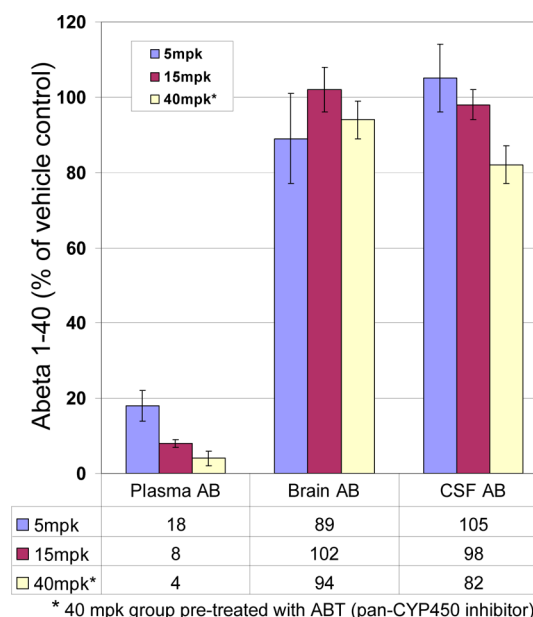


Figure 5. Levels of $A\beta$ 1–40 in the plasma, brain, and CSF of laboratory rats 5 h after sc administration of 5, 15, and 40 mg/kg doses of **22h**. All three doses of **22h** produced statistically significant reductions in plasma $A\beta$ levels relative to vehicle controls.

The source of the lack of $A\beta$ reduction in the brain and CSF is readily apparent in Figure 6: although high plasma

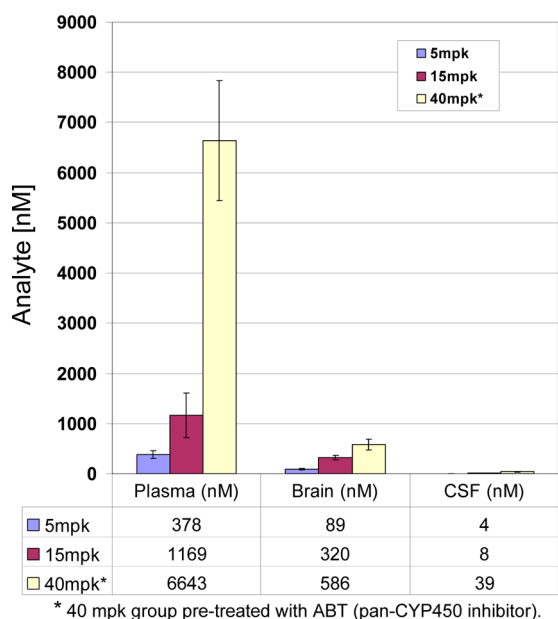


Figure 6. Levels of **22h** in the plasma, brain, and CSF of laboratory rats 5 h after sc administration of 5, 15, and 40 mg/kg doses of **22h**.

concentrations of **22h** were achieved, low drug levels were observed in the brain and CSF, independent of dose. As has been observed with many other BACE-1 ligands, the source of the low brain and CSF levels can be ascribed to P-glycoprotein (P-gp) efflux. To directly measure this effect, we utilized a cellular assay in which KBV cells (which express high levels of P-gp in comparison to HEK cells) were transfected with a plasmid that expressed APP containing the Swedish mutation.¹⁸ The KBV-Sw cellular assay was conducted with a representative group of acyl guanidines both in the presence and absence of the P-gp inhibitor tariquidar,²² as shown in Table 7. The effect

Table 7. Effect of P-gp Inhibition on KBV-Sw IC₅₀ Values for Representative Acyl Guanidines

compd	BACE-1 K _i (nM) ^a	KBV-Sw IC ₅₀ (nM) ^b	KBV-Sw + P-gp inhibitor IC ₅₀ (nM) ^c	P-gp shift ^d
8k	670	3300	3900	0.8
17d	60	1700	1030	1.7
17f	5	>10000	310	>32
22g	4	180	8	23
22h	5	180	5	36

^aMean radioligand displacement activity ($n \geq 2$) according to ref 7.

^b $A\beta$ lowering activity in KBV cells ($n \geq 2$) according to ref 18. ^cMean $A\beta$ lowering activity in the presence of 20 μ M P-gp inhibitor in KBV cells ($n \geq 2$) according to ref 18. ^dCalculated as the ratio of KBV-SW IC₅₀ values in the absence and presence of tariquidar (P-gp inhibitor).

of P-gp inhibition on the KBV-Sw IC₅₀ values (expressed as a ratio that we called the "P-gp shift") provided strong evidence that P-gp efflux was preventing the compound from inhibiting intracellular BACE-1 activity. It is striking that the initial acyl guanidine analogues (i.e., **8k** and **17d**) did not exhibit large P-gp shifts, but as BACE-1 binding potency increased, so did the magnitude of the P-gp shift. For example, the only difference between **17d** and **17f** is the addition of an acetyl group; this

minor modification produced a 10-fold increase in BACE-1 binding affinity and a 10-fold decrease in functional activity in KBV cells. All attempts to overcome this P-gp efflux issue while maintaining low nM BACE-1 activity were unsuccessful.

CONCLUSIONS

This work establishes the viability of the acyl guanidine functional group as an aspartyl protease active site isostere. By taking advantage of a previously developed route¹⁰ for the solid-phase synthesis of acyl guanidine libraries and the information gleaned from X-ray crystal structures, we rapidly optimized a micromolar HTS hit into a single digit nanomolar lead that afforded statistically significant reductions in peripheral $A\beta$ levels in rats 5 h after administration of a subcutaneous dose. Brain $A\beta$ levels were not reduced at any dose, most likely due to P-gp mediated efflux. X-ray crystallography of a representative acyl guanidine:BACE-1 complex revealed the unusual binding mode of this series; even though other BACE-1 inhibitors bearing acyl guanidine^{23–29} or acyl guanidine-like^{30–32} functional groups have been reported, none of them bind in the same orientation or exploit the same pattern of hydrogen binding interactions. Additional studies that explore the BACE-1 activity of macrocyclic isoxazolyl acyl guanidines will be reported in due course.

EXPERIMENTAL SECTION

General. Unless otherwise noted, all starting materials, reagents, and solvents were purchased from commercial vendors (Aldrich, VWR, Lancaster, etc.) and used as supplied without further purification. Wang resin was purchased from Polymer Laboratories. NMR spectra were recorded on a Bruker DPX-500, Bruker DPX-400, or Bruker DPX-300 NMR spectrometer. Chemical shifts are expressed in parts per million (δ) using a residual solvent proton as the internal standard. The following abbreviations are used to designate the multiplicities: s, singlet; d, doublet; t, triplet; q, quartet; m, multiplet. LC/MS analysis to assess final purity was performed on a Shimadzu HPLC equipped with a Phenomenex C18, 3.0 mm \times 50 mm column, a Micromass spectrometer, and eluting with a mixture of MeOH and H₂O containing 0.1% TFA with a gradient of 10–100% over 5 min. All samples provided HPLC purity (area% at 254 nm) \geq 95%. High resolution mass spectrometry (HRMS) analyses were performed on a Fourier Transform Orbitrap mass spectrometer (Exactone, Thermo Fisher Scientific, San Jose, CA) in positive or negative ionization electrospray mode operating at 25000 resolution (full width at half height maximum, fwhm). The instrument was daily calibrated according to manufacturer's specifications resulting in mass accuracy of or better than 5 ppm. The operating software Xcalibur was used to calculate theoretical mass-to-charge values and to process the obtained data.

General Procedure for Solid Phase Synthesis of Acyl Guanidines (Method A). Resin-Bound 4-Nitrophenylcarbonate Intermediate (2). To a suspension of Wang resin (50 g, 1.3 mmol/g, 65.0 mmol, 1.0 equiv) in 800 mL of anhydrous DCM was added 4-nitrophenyl chloroformate (39.3 g, 195.0 mmol, 3.0 equiv) and N-methylmorpholine (29.0 mL, 260 mmol, 4.0 equiv) at 25 °C. The resulting mixture was shaken at 25 °C overnight, then filtered and washed with DCM (4 \times 500 mL) and ether (2 \times 500 mL), and dried under house vacuum overnight to afford 74.5 g of **2**. Then 30 mg of the above resin was treated with 2 mL of 30% TFA in DCM for 1 h, then filtered. The filtrate was concentrated in vacuo to afford 5.1 mg of 4-nitrophenol, corresponding to a calculated loading of 1.2 mmol/g.

Resin-Bound S-Methylisothioureia Intermediate (3). To resin **2** (14 g, 16.8 mmol) suspended in 400 mL of DMF was added S-methylisothioureia sulfate (18.7 g, 67.2 mmol, 4.0 equiv) and cesium carbonate (21.9 g, 67.2 mmol, 4.0 equiv). The resulting suspension was shaken at room temperature for 2 d, then filtered, and the resin

was washed with DMF (3 × 200 mL), THF (3 × 200 mL), and MeOH (3 × 200 mL) and then dried in vacuo for 1 d to afford 14 g of **3**. Resin **3** was distributed into 400 Microkans (purchased from IRORI, 35 mg resin/Microkan, 42 μmol) and stored under nitrogen until needed.

Resin-Bound Acyl S-Methylthiourea Intermediate (5). To a reaction flask containing a Microkan loaded with resin **3** (35 mg, 42 μmol) was added NMP (2 mL), the appropriate isoxazole acid **4** (0.21 mmol, 5.0 equiv), PyAOP (0.21 mmol, 5.0 equiv), and DIEA (0.21 mmol, 5.0 equiv). The reaction flask was shaken at 25 °C for 24 h, filtered, and washed with DMF (3 × 2 mL), MeOH (3 × 2 mL), DCM (3 × 2 mL), and MeOH (3 × 2 mL) and then dried in vacuo overnight to afford a Microkan containing resin-bound acyl S-isothiurea **5** (35 mg, 42 μmol).

Resin-Bound Acyl Guanidine (7). To a flask containing a Microkan loaded with the appropriate acyl S-methylthiourea intermediate **5** (35 mg, 42 μmol) was added DCM (2 mL), DIEA (0.21 mmol, 5.0 equiv), and amine **6** (0.21 mmol, 5.0 equiv). The flask was shaken at 25 °C for 16 h, filtered, and washed with DCM (3 × 2 mL), MeOH (3 × 2 mL), then dried in vacuo overnight to afford a Microkan containing resin-bound acyl guanidine **7** (35 mg, 42 μmol).

Acyl Guanidines 1, 8a–8s. To a vial containing a Microkan loaded with the appropriate resin-bound acyl guanidine **7** (35 mg, 42 μmol) was added 50% TFA/DCM (2 mL), and the resulting suspension was shaken at 25 °C for 1 h. The Microkan was filtered and washed with 50% TFA/DCM (2 × 1 mL), and the combined TFA/DCM fractions were concentrated in vacuo and purified by preparative HPLC to afford compounds **1** and **8a–8s**.

N-(Amino(naphthalen-1-ylmethylamino)methylene)-5-methyl-3-phenylisoxazole-4-carboxamide (1). Compound **1** was prepared from **3** via method A using 5-methyl-3-phenylisoxazole-4-carboxylic acid as acid **4** and 1-naphthylmethylamine as amine **6**. Preparative HPLC purification afforded 7.7 mg (48% yield from **3**) of **1** as a white solid. ¹H NMR (500 MHz, CD₃OD) δ 7.99–7.96 (m, 4H), 7.69–7.60 (m, 3H), 7.55–7.53 (m, 5H), 5.04 (s, 2H), 2.70 (s, 3H). HRMS (ESI⁺): calculated for C₂₃H₂₁N₄O₂, [M + H]⁺ = 385.1659; observed, [M + H]⁺ = 385.1650.

N-(Amino(naphthalen-1-ylmethylamino)methylene)-3-(4-fluorophenyl)-5-methylisoxazole-4-carboxamide (8a). Compound **8a** was prepared from **3** via method A using 3-(4-fluorophenyl)-5-methylisoxazole-4-carboxylic acid as acid **4** and 1-naphthylmethylamine as amine **6**. Preparative HPLC purification afforded 9.7 mg (60% yield from **3**) of **8a** as an oil. ¹H NMR (500 MHz, CD₃OD) δ 8.03–7.88 (m, 4H), 7.73–7.54 (m, 5H), 7.24–7.19 (m, 2H), 5.05 (s, 2H), 2.70 (s, 3H). MS (ESI⁺) (m/z) 403.2 ([M + H]⁺).

N-(Amino(naphthalen-1-ylmethylamino)methylene)-3-(4-methoxyphenyl)-5-methylisoxazole-4-carboxamide (8b). Compound **8b** was prepared from **3** via method A using 3-(4-methoxy)-5-methylisoxazole-4-carboxylic acid as acid **4** and 1-naphthylmethylamine as amine **6**. Preparative HPLC purification afforded 5.6 mg (33% yield from **3**) of **8b** as a white solid. ¹H NMR (500 MHz, CD₃OD) δ 8.01–7.95 (m, 4H), 7.65–7.51 (m, 5H), 7.05–7.03 (m, 2H), 5.04 (s, 2H), 3.85 (s, 3H), 2.70 (s, 3H). MS (ESI⁺) (m/z) 414.1 ([M + H]⁺).

N-(Amino(benzylamino)methylene)-5-methyl-3-phenylisoxazole-4-carboxamide (8c). Compound **8c** was prepared from **3** via method A using 5-methyl-3-phenylisoxazole-4-carboxylic acid as acid **4** and benzylamine as amine **6**. Preparative HPLC purification afforded 9.6 mg (68% yield from **3**) of **8c** as a white solid. ¹H NMR (500 MHz, CD₃OD) δ 7.69 (d, J = 7.3 Hz, 2H), 7.53 (d, J = 7.3 Hz, 3H), 7.42–7.38 (m, 5H), 4.58 (s, 2H), 2.71 (s, 3H). MS (ESI⁺) (m/z) 335.2 ([M + H]⁺).

N-(Amino(benzylamino)methylene)-5-methyl-3-(4-fluorophenyl)-isoxazole-4-carboxamide (8d). Compound **8d** was prepared from **3** via method A using 3-(4-fluorophenyl)-5-methylisoxazole-4-carboxylic acid as acid **4** and benzylamine as amine **6**. Preparative HPLC purification afforded 10.9 mg (74% yield from **3**) of **8d** as a white solid. ¹H NMR (500 MHz, CD₃OD) δ 7.69 (d, J = 7.3 Hz, 2H), 7.53 (d, J = 7.3 Hz, 2H), 7.42–7.38 (m, 5H), 4.58 (s, 2H), 2.71 (s, 3H). MS (ESI⁺) (m/z) 353.3 ([M + H]⁺).

N-(Amino(benzylamino)methylene)-5-methyl-3-(4-methoxyphenyl)isoxazole-4-carboxamide (8e). Compound **8e** was prepared from **3** via method A using 3-(4-methoxyphenyl)-5-methylisoxazole-4-carboxylic acid as acid **4** and benzylamine as amine **6**. Preparative HPLC purification afforded 2.5 mg (16% yield from **3**) of **8e** as a white solid. ¹H NMR (500 MHz, CD₃OD) δ 7.63 (d, J = 7.4 Hz, 2H), 7.44–7.42 (m, 2H), 7.39 (d, J = 7.2 Hz, 2H), 4.58 (s, 2H), 3.87 (s, 3H), 2.69 (s, 3H). MS (ESI⁺) (m/z) 365.1 ([M + H]⁺).

N-(Amino(3,4-dichlorobenzylamino)methylene)-5-methyl-3-phenylisoxazole-4-carboxamide (8f). Compound **8f** was prepared from **3** via method A using 5-methyl-3-phenylisoxazole-4-carboxylic acid as acid **4** and 3,4-dichlorobenzylamine as amine **6**. Preparative HPLC purification afforded 15.1 mg (89% yield from **3**) of **8f** as an oil. ¹H NMR (500 MHz, CD₃OD) δ 7.69–7.63 (m, 2H), 7.56–7.52 (m, 5H), 7.32 (s, 1H), 4.58 (s, 2H), 2.72 (s, 3H). MS (ESI⁺) (m/z) 403.1 ([M + H]⁺).

N-(Amino(3,4-dichlorobenzylamino)methylene)-5-methyl-3-(4-fluorophenyl)isoxazole-4-carboxamide (8g). Compound **8g** was prepared from **3** via method A using 3-(4-fluorophenyl)-5-methylisoxazole-4-carboxylic acid as acid **4** and 3,4-dichlorobenzylamine as amine **6**. Preparative HPLC purification afforded 3.4 mg (19% yield from **3**) of **8g** as an oil. ¹H NMR (300 MHz, CD₃OD) δ 7.77–7.72 (m, 2H), 7.61–7.58 (m, 2H), 7.29–7.23 (m, 3H), 4.58 (s, 2H), 2.71 (s, 3H). MS (ESI⁺) (m/z) 421.1 ([M + H]⁺).

N-(Amino(3,4-dichlorobenzylamino)methylene)-5-methyl-3-(4-methoxyphenyl)isoxazole-4-carboxamide (8h). Compound **8h** was prepared from **3** via method A using 3-(4-methoxyphenyl)-5-methylisoxazole-4-carboxylic acid as acid **4** and 3,4-dichlorobenzylamine as amine **6**. Preparative HPLC purification afforded 3.1 mg (17% yield from **3**) of **8h** as an oil. ¹H NMR (500 MHz, CD₃OD) δ 7.64–7.57 (m, 4H), 7.33–7.31 (m, 1H), 7.06 (d, J = 8.7 Hz, 2H), 4.58 (s, 2H), 3.86 (s, 3H), 2.71 (s, 3H). MS (ESI⁺) (m/z) 433.1 ([M + H]⁺).

N-(Amino(3,5-dichlorobenzylamino)methylene)-5-methyl-3-phenylisoxazole-4-carboxamide (8i). Compound **8i** was prepared from **3** via method A using 5-methyl-3-phenylisoxazole-4-carboxylic acid as acid **4** and 3,5-dichlorobenzylamine as amine **6**. Preparative HPLC purification afforded 9.6 mg (57% yield from **3**) of **8i** as a white solid. ¹H NMR (300 MHz, CD₃OD) δ 7.69 (d, J = 6.1 Hz, 2H), 7.55–7.53 (m, 3H), 7.48 (s, 1H), 7.37 (s, 2H), 4.59 (s, 2H), 2.72 (s, 3H). MS (ESI⁺) (m/z) 403.1 ([M + H]⁺).

N-(Amino(3,5-dichlorobenzylamino)methylene)-5-methyl-3-(4-fluorophenyl)isoxazole-4-carboxamide (8j). Compound **8j** was prepared from **3** via method A using 3-(4-fluorophenyl)-5-methylisoxazole-4-carboxylic acid as acid **4** and 3,5-dichlorobenzylamine as amine **6**. Preparative HPLC purification afforded 4.6 mg (26% yield from **3**) of **8j** as a white solid. ¹H NMR (500 MHz, CD₃OD) δ 7.75 (dd, J = 8.5 Hz, J = 5.7 Hz, 2H), 7.48 (s, 1H), 7.38 (s, 2H), 7.27 (t, J = 8.1 Hz, 2H), 4.60 (s, 2H), 2.72 (s, 3H). MS (ESI⁺) (m/z) 421.1 ([M + H]⁺).

N-(Amino(3,5-dichlorobenzylamino)methylene)-5-methyl-3-(4-methoxyphenyl)isoxazole-4-carboxamide (8k). Compound **8k** was prepared from **3** via method A using 3-(4-methoxyphenyl)-5-methylisoxazole-4-carboxylic acid as acid **4** and 3,4-dichlorobenzylamine as amine **6**. Preparative HPLC purification afforded 15 mg (83% yield from **3**) of **8k** as a white solid. ¹H NMR (500 MHz, CD₃OD) δ 7.64 (d, J = 7.0 Hz, 2H), 7.48 (s, 1H), 7.37 (s, 2H), 7.07 (d, J = 7.0 Hz, 2H), 4.59 (s, 2H), 3.87 (s, 3H), 2.70 (s, 3H). HRMS (ESI⁺): calculated for C₂₀H₁₉N₄O₃Cl₂, [M + H]⁺ = 433.0829; observed, [M + H]⁺ = 433.0818.

N-(Amino(3,5-dichlorobenzylamino)methylene)-3-methyl-5-(4-methoxyphenyl)isoxazole-4-carboxamide (8l). Compound **8l** was prepared from **3** via method A using 3-methyl-5-(4-methoxyphenyl)isoxazole-4-carboxylic acid as acid **4** and 3,5-dichlorobenzylamine as amine **6**. Preparative HPLC purification afforded 15.7 mg (86% yield from **3**) of **8l** as an off-white solid. ¹H NMR (500 MHz, CD₃OD) δ 7.81 (d, J = 8.6 Hz, 2H), 7.49 (s, 1H), 7.39 (s, 2H), 7.13 (d, J = 8.6 Hz, 2H), 4.61 (s, 2H), 3.90 (s, 3H), 2.46 (s, 3H). MS (ESI⁺) (m/z) 433.1 ([M + H]⁺).

N-(Amino(3,5-dichlorobenzylamino)methylene)-3-(4-methoxyphenyl)-5-methyl-1*H*-pyrazole-4-carboxamide (**8m**). Compound **8m** was prepared from **3** via method A using 3-(4-methoxyphenyl)-5-methyl-1*H*-pyrazole-4-carboxylic acid as acid **4** and 3,5-dichlorobenzylamine as amine **6**. Preparative HPLC purification afforded 3.8 mg (21% yield from **3**) of **8m** as an oil. ¹H NMR (500 MHz, CD₃OD) δ 7.56 (d, *J* = 8.5 Hz, 2H), 7.48 (s, 1H), 7.35 (s, 2H), 7.06 (d, *J* = 8.5 Hz, 2H), 4.61 (s, 2H), 3.85 (s, 3H), 2.51 (s, 3H). MS (ESI+) (*m/z*) 432.1 ([*M* + H]⁺).

N-(Amino(3,5-dichlorobenzylamino)methylene)-5-(4-methoxyphenyl)-1,3-dimethyl-1*H*-pyrazole-4-carboxamide (**8n**). Compound **8n** was prepared from **3** via method A using 5-(4-methoxyphenyl)-1,3-dimethyl-1*H*-pyrazole-4-carboxylic acid as acid **4** and 3,5-dichlorobenzylamine as amine **6**. Preparative HPLC purification afforded 3.5 mg (19% yield from **3**) of **8n** as an oil. ¹H NMR (500 MHz, CD₃OD) δ 7.47–7.43 (m, 4H), 7.31 (s, 1H), 7.11 (d, *J* = 8.75 Hz, 2H), 4.61 (s, 2H), 3.72 (s, 3H), 2.84 (s, 3H), 2.46 (s, 3H). MS (ESI+) (*m/z*) 446.1 ([*M* + H]⁺).

N-(Amino(3,5-dichlorobenzylamino)methylene)-3-(4-methoxyphenyl)-5-methylisothiazole-4-carboxamide (**8o**). Compound **8o** was prepared from **3** via method A using 3-(4-methoxyphenyl)-5-methylisothiazole-4-carboxylic acid as acid **4** and 3,5-dichlorobenzylamine as amine **6**. Preparative HPLC purification afforded 11.6 mg (62% yield from **3**) of **8o** as a white solid. ¹H NMR (500 MHz, CD₃OD) δ 7.60 (d, *J* = 8.78 Hz, 2H), 7.47–7.46 (m, 1H), 7.33 (s, 2H), 7.02 (d, *J* = 8.8 Hz, 2H), 4.59 (s, 2H), 3.84 (s, 3H), 2.73 (s, 3H). MS (ESI+) (*m/z*) 449.0 ([*M* + H]⁺).

N-(Amino(naphthalen-1-ylmethylamino)methylene)-3-(4-methoxyphenyl)-5-methylisothiazole-4-carboxamide (**8p**). Compound **8p** was prepared from **3** via method A using 3-(4-methoxyphenyl)-5-methylisothiazole-4-carboxylic acid as acid **4** and 1-naphthylmethylamine as amine **6**. Preparative HPLC purification afforded 14 mg (77% yield from **3**) of **8p** as a white solid. ¹H NMR (500 MHz, CD₃OD) δ 8.0–7.93 (m, 3H), 7.67–7.48 (m, 6H), 7.02–6.99 (m, 2H), 5.05 (s, 2H), 3.86 (s, 3H), 2.73 (s, 3H). MS (ESI+) (*m/z*) 431.2 ([*M* + H]⁺).

N-(Amino(naphthalen-2-ylmethylamino)methylene)-3-(4-methoxyphenyl)-5-methylisothiazole-4-carboxamide (**8q**). Compound **8q** was prepared from **3** via method A using 3-(4-methoxyphenyl)-5-methylisothiazole-4-carboxylic acid as acid **4** and 2-naphthylmethylamine as amine **6**. Preparative HPLC purification afforded 2.7 mg (15% yield from **3**) of **8q** as a white solid. ¹H NMR (500 MHz, CD₃OD) δ 8.0–7.93 (m, 3H), 7.67–7.48 (m, 6H), 7.02–6.99 (m, 2H), 5.05 (s, 2H), 3.86 (s, 3H), 2.73 (s, 3H). MS (ESI+) (*m/z*) 431.2 ([*M* + H]⁺).

N-(Amino(3-chloro-5-bromobenzylamino)methylene)-3-(4-methoxyphenyl)-5-methylisothiazole-4-carboxamide (**8r**). Compound **8r** was prepared from **3** via method A using 3-(4-methoxyphenyl)-5-methylisothiazole-4-carboxylic acid as acid **4** and 3-chloro-5-bromobenzylamine as amine **6**. Preparative HPLC purification afforded 5.8 mg (20% yield from **3**) of **8r** as a white solid. ¹H NMR (500 MHz, MeOD) δ 7.3 (m, 3H), 7.49 (s, 1H), 7.38 (s, 1H), 7.04 (d, *J* = 8.5 Hz, 2H), 4.59 (s, 2H), 3.85 (s, 3H), 2.74 (s, 3H). MS (ESI+) (*m/z*) 492.92, 494.92 ([*M* + H]⁺).

N-(Amino(3,5-dimethylbenzylamino)methylene)-3-(4-methoxyphenyl)-5-methylisothiazole-4-carboxamide (**8s**). Compound **8s** was prepared from **3** via method A using 3-(4-methoxyphenyl)-5-methylisothiazole-4-carboxylic acid as acid **4** and 3,5-dimethylbenzylamine as amine **6**. Preparative HPLC purification afforded 2.7 mg (15% yield from **3**) of **8s** as a white solid. ¹H NMR (500 MHz, CD₃OD) δ 7.60 (d, *J* = 8.5 Hz, 2H), 7.03–6.98 (m, 3H), 6.94 (br s, 2H), 4.47 (br s, 2H), 3.83 (s, 3H), 2.71 (d, *J* = 0.9 Hz, 3H), 2.32 (s, 6H). MS (ESI+) (*m/z*) 409.2 ([*M* + H]⁺).

General Procedure for Solution Phase Synthesis of Acyl Guanidines (Method B). *tert*-Butyl Methylthiocarbonylcarbamate (**12**). To a vigorously stirred suspension of *S*-methylisothiourea hemisulfate (60.8 g, 0.437 mol) in CH₂Cl₂ (600 mL) was added 2*N* NaOH (300 mL, 0.6 mol). This was cooled to 0 °C on an ice bath, and a solution of di-*tert*-butyl dicarbonate (43.2 g, 0.198 mol) was added dropwise over 6 h. Upon completion of the addition, the mixture was stirred an additional 20 min and diluted with 1 L CH₂Cl₂, and the phases were separated. The organic portion was washed with water (2

× 500 mL) and dried over Na₂SO₄. Filtration and concentration provided *tert*-butyl methylthiocarbonylcarbamate (**12**) as a white solid (35.5 g, 0.187 mol, 94% yield based on Boc₂O). ¹H NMR (500 MHz, CDCl₃) δ 2.47 (s, 3H), 1.52 (s, 9H).

tert-Butyl *N*-(3-(4-methoxyphenyl)-5-methylisoxazole-4-carbonyl)(methylthio)carbonylcarbamate (**14a**). A mixture of *tert*-butyl methylthiocarbonylcarbamate (0.98 g, 5.15 mmol), 3-(4-methoxyphenyl)-5-methyl-4-isoxazolecarboxylic acid (1.17 g, 5.02 mmol), EDCI (1.20 g, 6.26 mmol), and DMAP (1.22 g, 10.0 mmol) in DCM (30 mL) was stirred for 3 h. The solvent was evaporated by a rotary evaporator and residue was purified by flash chromatography (DCM, R_f 0.38). The product **14a** was obtained as a white solid (1.2 g, 60% yield). ¹H NMR (500 MHz, CD₃OD) δ 7.46 (d, *J* = 8.9 Hz, 2H), 6.99 (d, *J* = 8.5 Hz, 2H), 3.84 (s, 3H), 2.74 (s, 3H), 1.87 (s, 3H), 1.50 (s, 9H). MS (ESI+) (*m/z*) 406 ([*M* + H]⁺).

tert-Butyl *N*-(3-(4-methoxyphenyl)-5-methylisothiazole-4-carbonyl)(methylthio)carbonylcarbamate (**14b**). Compound **14b** was synthesized by analogy to the preparation of **14a**, substituting 3-(4-methoxyphenyl)-5-methyl-4-isothiazolecarboxylic acid for 3-(4-methoxyphenyl)-5-methyl-4-isoxazolecarboxylic acid to afford **14b** as a white solid. ¹H NMR (400 MHz, CDCl₃) δ 12.36 (s, 1H), 7.46 (d, *J* = 8.8 Hz, 2H), 6.92 (d, *J* = 8.8 Hz, 2H), 3.84 (s, 3H), 2.75 (s, 3H), 1.72 (s, 3H), 1.53 (s, 9H). MS (ESI+) (*m/z*) 422 ([*M* + H]⁺).

General Procedure for the Preparation of BOC-Protected Acyl Guanidine (16). The reaction mixture of 20 mg of *tert*-butyl *N*-(3-(4-methoxyphenyl)-5-methylisothiazole-4-carbonyl)(methylthio)carbonylcarbamate (**14b**), 23 mg of amine **15**, and 0.030 mL of DIEA in 4 mL of DCM was stirred at room temperature overnight and then concentrated in vacuo to afford **16** as a crude product.

General Procedure for the Preparation of Acyl Guanidine (17). Intermediate **16** was treated with 0.5 mL of 50% TFA in DCM at room temperature for 1 h. The reaction mixture was concentrated in vacuo, and the product was purified by preparative HPLC (0.1% TFA MeOH/H₂O) to afford acyl guanidine **17**.

N-(3-(4-methoxyphenyl)-5-methylisothiazole-4-carbonyl)(methylthio)carbonylcarbamate (**16a**). A mixture of **14b** (0.830 g, 1.97 mmol), 3,5-dichloro-4-aminobenzylamine (0.450 g, 2.36 mmol), and DIPEA (0.61 g, 4.72 mmol) in DCM (20 mL) was stirred at room temperature overnight. Water (100 mL) and DCM (80 mL) were added to the reaction mixture, and the solution was transferred to a separatory funnel. The two layers were separated, and the aqueous solution was extracted with 100 mL of DCM. The combined extract was dried over anhydrous sodium sulfate and then filtered and concentrated in vacuo. The crude product was purified by flash chromatography (DCM, R_f 0.21) to give 0.920 g (83% yield) of **16a** as a white solid. ¹H NMR (500 MHz, CDCl₃) δ 12.09 (s, 1H), 8.58 (s, 1H), 7.50 (d, *J* = 8.7 Hz, 2H), 6.95 (s, 2H), 6.88 (d, *J* = 8.7 Hz, 2H), 4.43 (s, 2H), 3.90 (d, *J* = 5.5 Hz, 2H), 3.77 (s, 3H), 2.69 (s, 3H), 1.49 (s, 9H). MS (ESI+) (*m/z*) 564 ([*M* + H]⁺).

tert-Butyl *N*-(4-amino-3-chloro-5-methylbenzyl)-*N'*-(3-(4-methoxyphenyl)-5-methylisothiazole-4-carbonyl)carbonylcarbamate (**16b**). Compound **16b** (1.97 g) was prepared by analogy to **16a**, substituting 4-(aminomethyl)-2-chloro-6-methylaniline for 3,5-dichloro-4-aminobenzylamine to afford 1.94 g (79% yield) of **16b** as white solid. ¹H NMR (CDCl₃, 500 MHz) δ 12.09 (s, 1H), 8.53 (s, 1H), 7.52 (d, *J* = 8.6 Hz, 2H), 6.93 (s, 1H), 6.89 (d, *J* = 8.6 Hz, 2H), 6.74 (s, 1H), 4.00 (s, 2H), 3.92 (d, *J* = 5.5 Hz, 2H), 3.77 (s, 3H), 2.70 (s, 3H), 2.16 (s, 3H), 1.48 (s, 9H). MS (ESI+) (*m/z*) 544 ([*M* + H]⁺).

N-(Amino(3,5-dichloro-4-hydroxybenzylamino)methylene)-3-(4-methoxyphenyl)-5-methylisothiazole-4-carboxamide (**17a**). Compound **17a** was prepared from **3** via method A using 3-(4-methoxyphenyl)-5-methylisothiazole-4-carboxylic acid as acid **4** and 3,5-dichloro-4-hydroxybenzylamine as amine **6**. Preparative HPLC purification afforded 5.6 mg (10% yield from **3**) of **17a** as a white solid. ¹H NMR (500 MHz, CD₃OD) δ 7.62 (d, *J* = 7.8 Hz, 2H), 7.42 (s, 2H), 7.07 (d, *J* = 7.8 Hz, 2H), 4.46 (s, 2H), 3.86 (s, 3H), 2.68 (s, 3H). MS (ESI+) (*m/z*) 449.1 ([*M* + H]⁺).

N-(Amino(3,5-dichloro-4-propoxybenzylamino)methylene)-3-(4-methoxyphenyl)-5-methylisothiazole-4-carboxamide (**17b**).

Compound **17b** was prepared from **3** via method A using 3-(4-methoxyphenyl)-5-methylisothiazole-4-carboxylic acid as acid **4** and 3,5-dichloro-4-propoxybenzylamine as amine **6**. Preparative HPLC purification afforded 20 mg (32% yield from **3**) of **17b** as a white solid. $^1\text{H NMR}$ (500 MHz, CD_3OD) δ 7.64 (d, $J = 7.6$ Hz, 2H), 7.42 (s, 2H), 7.07 (d, $J = 7.9$ Hz, 2H), 4.53 (s, 2H), 4.02 (t, $J = 6.4$ Hz, 2H), 3.87 (s, 3H), 2.69 (s, 3H), 1.84–1.90 (m, 2H), 1.12 (t, 3H, $J = 7.5$ Hz, 3H). MS (ESI+) (m/z) 491.1 ($[\text{M} + \text{H}]^+$).

N-(Amino(4-amino-3,5-dichlorobenzylamino)methylene)-3-(4-methoxyphenyl)-5-methylisoxazole-4-carboxamide (**17c**). Compound **17c** was prepared from **14a** via method B using 3,5-dichloro-4-aminobenzylamine as amine **15**. Preparative HPLC purification afforded 11 mg (47% yield from **14a**) of **17c** as a white solid. $^1\text{H NMR}$ (500 MHz, CD_3OD) δ 7.60 (d, $J = 8.8$ Hz, 2H), 7.24 (s, 2H), 7.03 (d, $J = 8.6$ Hz, 2H), 4.39 (s, 2H), 3.84 (s, 3H), 2.66 (s, 3H). MS (ESI+) (m/z) 448 ($[\text{M} + \text{H}]^+$).

N-(Amino(4-amino-3,5-dichlorobenzylamino)methylene)-3-(4-methoxyphenyl)-5-methylisothiazole-4-carboxamide (**17d**). Compound **17d** was prepared from **14b** via method B using 3,5-dichloro-4-aminobenzylamine as amine **15**. Preparative HPLC purification afforded 13 mg (45% yield from **14b**) of **17d** as a white solid. $^1\text{H NMR}$ (500 MHz, CD_3OD) δ 7.60 (d, $J = 8.6$ Hz, 2H), 7.22 (s, 2H), 7.00 (d, $J = 8.8$ Hz, 2H), 4.39 (s, 2H), 3.83 (s, 3H), 2.71 (s, 3H). HRMS (ESI+): calculated for $\text{C}_{20}\text{H}_{20}\text{N}_5\text{O}_2\text{Cl}_2\text{S}$, $[\text{M} + \text{H}]^+ = 464.0709$; observed, $[\text{M} + \text{H}]^+ = 464.0697$.

N-((4-Acetamido-3,5-dichlorobenzylamino)(amino)methylene)-3-(4-methoxyphenyl)-5-methylisoxazole-4-carboxamide (**17e**). Compound **17e** was prepared from **14a** via method B using 3,5-dichloro-4-acetamidobenzylamine as amine **15**. Preparative HPLC purification afforded 12.1 mg (78% yield from **14a**) of **17e** as a white solid. $^1\text{H NMR}$ (400 MHz, CDCl_3) δ 7.50 (d, $J = 7.8$ Hz, 2H), 7.22 (s, 2H), 6.92 (d, $J = 8.3$ Hz, 2H), 4.42 (s, 2H), 3.79 (s, 3H), 2.69 (s, 3H), 2.18 (s, 3H). MS (ESI+) (m/z) 491 ($[\text{M} + \text{H}]^+$).

N-((4-Acetamido-3,5-dichlorobenzylamino)(amino)methylene)-3-(4-methoxyphenyl)-5-methylisothiazole-4-carboxamide (**17f**). Compound **17f** was prepared from **14b** via method B using 3,5-dichloro-4-acetamidobenzylamine as amine **15**. Preparative HPLC purification afforded 64.5 mg (84% yield from **14b**) of **17f** as a white solid. $^1\text{H NMR}$ (500 MHz, CD_3OD) δ 7.60 (d, $J = 8.6$ Hz, 2H), 7.43 (s, 2H), 7.02 (d, $J = 8.8$ Hz, 2H), 4.39 (s, 2H), 3.83 (s, 3H), 2.72 (s, 3H), 2.19 (s, 3H). HRMS (ESI+): calculated for $\text{C}_{22}\text{H}_{22}\text{N}_5\text{O}_3\text{Cl}_2\text{S}$, $[\text{M} + \text{H}]^+ = 506.0815$; observed, $[\text{M} + \text{H}]^+ = 506.0805$.

N-((4-Acetamido-3-chloro-5-methylbenzylamino)(amino)methylene)-3-(4-methoxyphenyl)-5-methylisothiazole-4-carboxamide (**17g**). Compound **17g** was prepared from **14b** via method B using *N*-(4-(aminomethyl)-2-chloro-6-methylphenyl)acetamide as amine **15**. Preparative HPLC purification afforded 17.4 mg (72% yield from **3**) of **17g** as a white solid. $^1\text{H NMR}$ (500 MHz, CD_3OD) δ 7.60 (d, $J = 8.5$ Hz, 2H), 7.30 (br s, 1H), 7.17 (br s, 1H), 7.01 (d, $J = 8.9$ Hz, 2H), 4.53 (br s, 2H), 3.83 (s, 3H), 2.71 (s, 3H), 2.27 (s, 3H), 2.18 (s, 3H). HRMS (ESI+): calculated for $\text{C}_{23}\text{H}_{25}\text{N}_5\text{O}_3\text{ClS}$, $[\text{M} + \text{H}]^+ = 486.1361$; observed, $[\text{M} + \text{H}]^+ = 486.1349$.

N-(Amino(3,5-dichloro-4-(methylsulfonamido)benzylamino)methylene)-3-(4-methoxyphenyl)-5-methylisothiazole-4-carboxamide (**17h**). Compound **17h** was prepared from **14b** via method B using 3,5-dichloro-4-(methylsulfonamido)benzylamine as amine **15**. Preparative HPLC purification afforded 11.8 mg (27% yield from **14b**) of **17h** as a white powder. $^1\text{H NMR}$ (500 MHz, CD_3OD) δ 7.60 (d, $J = 8.5$ Hz, 2H), 7.45 (br s, 2H), 7.02 (d, $J = 8.5$ Hz, 2H), 4.57 (br s, 2H), 3.83 (d, $J = 3.4$ Hz, 3H), 3.23 (s, 3H), 2.70–2.74 (m, 3H). MS (ESI+) (m/z) 542 ($[\text{M} + \text{H}]^+$).

N-(Amino(3-chloro-5-methyl-4-propionamidobenzylamino)methylene)-3-(4-methoxyphenyl)-5-methylisoxazole-4-carboxamide (**17i**). Compound **17i** was prepared from **14a** via method B using 3-chloro-5-methyl-4-propionamidobenzylamine as amine **15**. Preparative HPLC purification afforded 11.1 mg (46% yield from **14a**) of **17i** as a white solid. $^1\text{H NMR}$ (400 MHz, CD_3OD) δ 7.61 (d, $J = 8.8$ Hz, 2H), 7.33 (s, 1H), 7.21 (s, 1H), 7.04 (d, $J = 8.8$ Hz, 2H), 4.53 (s, 2H), 3.84 (s, 3H), 2.67 (s, 3H), 2.46 (q, $J = 7.5$ Hz, 2H), 2.26 (s, 3H), 1.26 (t, 3H). MS (ESI+) (m/z) 484 ($[\text{M} + \text{H}]^+$).

N-(Amino(4-benzamido-3-chloro-5-methylbenzylamino)methylene)-3-(4-methoxyphenyl)-5-methylisothiazole-4-carboxamide (**17j**). Compound **17j** was prepared from **14b** via method B using 4-benzamido-3-chloro-5-methylbenzylamine as amine **15**. Preparative HPLC purification afforded 17.2 mg (67% yield from **14b**) of **17j** as a white powder. $^1\text{H NMR}$ (400 MHz, CD_3OD) δ 7.97–8.03 (m, 2H), 7.59–7.67 (m, 3H), 7.51–7.58 (m, 2H), 7.36 (br s, 1H), 7.24 (br s, 1H), 7.00–7.07 (m, 2H), 4.58 (br s, 2H), 3.83 (s, 3H), 2.73 (s, 3H), 2.34 (s, 3H). MS (ESI+) (m/z) 548 ($[\text{M} + \text{H}]^+$).

N-(Amino(3,5-dichloro-4-(2-(methylthio)acetamido)benzylamino)methylene)-3-(4-methoxyphenyl)-5-methylisoxazole-4-carboxamide (**17k**). **Step 1.** *N*-((4-Amino-3,5-dichlorobenzylamino)(*tert*-butoxycarbonylamino)methylene)-3-(4-methoxyphenyl)-5-methylisoxazole-4-carboxamide. A mixture of **14a** (2.10 g, 5.18 mmol), 3,5-dichloro-4-aminobenzylamine (1.20 g, 6.28 mmol), and DIPEA (1.80 mL, 10.3 mmol) in DCM (40 mL) was stirred at room temperature overnight. Water (200 mL) and DCM (160 mL) were added to the reaction mixture, and the solution was transferred to a separatory funnel. The two layers were separated, and the aqueous solution was extracted with 150 mL of DCM. The combined extract was dried over anhydrous sodium sulfate, then filtered and concentrated in vacuo. The crude product was purified by flash chromatography (DCM, R_f 0.25) to give 2.78 g (98% yield) of the title compound as a white solid. $^1\text{H NMR}$ (500 MHz, CDCl_3) δ 12.18 (s, 1H), 8.67 (br s, 1H), 7.53 (d, $J = 8.5$ Hz, 2H), 6.96 (s, 2H), 6.90 (d, $J = 8.2$ Hz, 2H), 4.45 (br s, 2H), 4.03 (d, $J = 5.8$ Hz, 2H), 3.77 (s, 3H), 2.73 (s, 3H), 1.49 (s, 9H). MS (ESI+) (m/z) 548 ($[\text{M} + \text{H}]^+$).

Step 2. *N*-((4-(2-Bromoacetamido)-3,5-dichlorobenzylamino)(*tert*-butoxycarbonylamino)methylene)-3-(4-methoxyphenyl)-5-methylisoxazole-4-carboxamide (isoxazole analogue of **20a**). *N*-((4-Amino-3,5-dichlorobenzylamino)(*tert*-butoxycarbonylamino)methylene)-3-(4-methoxyphenyl)-5-methylisoxazole-4-carboxamide (1.23 g, 2.24 mmol) was dissolved in 20 mL of anhydrous DCM in a 250 mL round-bottom flask, followed by the addition of 0.343 mL (2.46 mmol, 1.1 equiv) of triethylamine. The solution was cooled to 0 °C, and nitrogen was introduced. Bromoacetyl bromide (0.214 mL, 2.46 mmol, 1.1 equiv) was added dropwise, and the reaction mixture was stirred at 0 °C for 1 h. More bromoacetyl bromide (0.100 mL) was added, and the reaction mixture was stirred at 0 °C for 1 h. DCM (80 mL) and saturated NaHCO_3 aqueous solution (100 mL) were added, and the layers were separated. The aqueous was extracted with DCM (50 mL). The combined organic extracts were dried over anhydrous sodium sulfate. The crude product was purified by flash chromatography (EtOAc/DCM, 5:95, R_f 0.34) to give 1.43 g (96% yield) of the title compound as a white solid. $^1\text{H NMR}$ (500 MHz, CDCl_3) δ 12.20 (s, 1H), 8.84 (t, $J = 5.6$ Hz, 1H), 7.91 (br s, 1H), 7.53–7.46 (m, 2H), 7.11 (s, 2H), 6.88 (d, $J = 8.9$ Hz, 2H), 4.11 (d, $J = 5.8$ Hz, 2H), 4.09 (s, 2H), 3.79 (s, 3H), 2.70 (s, 3H), 1.51 (s, 9H). MS (ESI+) (m/z) 668 ($[\text{M} + \text{H}]^+$).

Step 3. *N*-((*tert*-butoxycarbonylamino)(3,5-dichloro-4-(2-(methylthio)acetamido)benzylamino)methylene)-3-(4-methoxyphenyl)-5-methylisoxazole-4-carboxamide (BOC-**17k**). The mixture of 147 mg (0.506 mmol) of 1,3-di-Boc-2-methylisothiourea, 24 mg (0.406 mmol) of *n*-propylamine, and 0.088 mL (0.051 mmol) of DIPEA in 1.5 mL of DCM was stirred at room temperature overnight to generate methanethiolate in situ. *N*-((4-(2-Bromoacetamido)-3,5-dichlorobenzylamino)(*tert*-butoxycarbonylamino)methylene)-3-(4-methoxyphenyl)-5-methylisoxazole-4-carboxamide (100 mg, 0.149 mmol) was added to the reaction mixture, which was stirred at room temperature for 16 h. The reaction mixture was washed with water and solvent was evaporated in vacuo to give the crude product of *N*-((*tert*-butoxycarbonylamino)(3,5-dichloro-4-(2-(methylthio)acetamido)benzylamino)methylene)-3-(4-methoxyphenyl)-5-methylisoxazole-4-carboxamide (BOC-**17k**). To half of the crude product was added 1.0 mL of 50% TFA in DCM, and the resulting solution was stirred at RT for 1 h. The solution was concentrated in vacuo, and the product was purified by preparative HPLC (0.1% TFA, MeOH/water) to give 15 mg (36% yield) of title compound. $^1\text{H NMR}$ (500 MHz, CD_3OD) δ 7.61 (d, $J = 8.2$ Hz, 2H), 7.48 (br s, 2H), 7.04 (d, $J = 8.2$

H₂, 2H), 4.58 (br s, 2H), 3.84 (s, 3H), 3.38 (s, 2H), 2.67 (s, 3H), 2.28 (s, 3H). MS (ESI+) (*m/z*) 536 ([M + H]⁺).

N-(Amino(3-chloro-5-methyl-4-(3-(methylthio)propanamido)benzylamino)methylene)-3-(4-methoxyphenyl)-5-methylisoxazole-4-carboxamide (**17l**). Compound **17l** was prepared from **14a** via method B using 3-chloro-5-methyl-4-(3-(methylthio)propanamido)benzylamine as amine **15**. Preparative HPLC purification afforded 6.1 mg (24% yield from **14a**) of **17l** as a white solid. ¹H NMR (400 MHz, CD₃OD) δ 7.62 (d, *J* = 8.8 Hz, 2H), 7.34 (br s, 1H), 7.21 (br s, 1H), 7.05 (d, *J* = 8.8 Hz, 2H), 4.53 (br s, 2H), 3.85 (s, 3H), 2.89–2.83 (m, 2H), 2.78–2.72 (m, 2H), 2.68 (s, 3H), 2.30 (s, 3H), 2.17 (s, 3H). MS (ESI+) (*m/z*) 530 ([M + H]⁺).

N-(Amino(3,5-dichloro-4-(2-(methylsulfonyl)acetamido)benzylamino)methylene)-3-(4-methoxyphenyl)-5-methylisoxazole-4-carboxamide (**17m**). *N*-((*tert*-Butoxycarbonylamino)(3,5-dichloro-4-(2-(methylthio)acetamido)benzylamino)methylene)-3-(4-methoxyphenyl)-5-methylisoxazole-4-carboxamide (BOC-**17k**) (64 mg of crude product) and 47 mg of mCPBA in 2 mL of DCM was stirred at room temperature overnight. Solvent was evaporated, and the residue was treated with 1.0 mL of 50% TFA in DCM at room temperature for 1 h. Solvent and TFA were evaporated in vacuo. The product was purified by preparative HPLC (0.1% TFA, MeOH/water) to give 6.4 mg (15% yield) of title compound. ¹H NMR (500 MHz, CD₃OD) δ 7.62 (d, *J* = 8.9 Hz, 2H), 7.49 (br s, 2H), 7.05 (d, *J* = 8.9 Hz, 2H), 4.59 (br s, 2H), 4.31 (s, 2H), 3.84 (s, 3H), 3.19 (s, 3H), 2.68 (s, 3H). MS (ESI+) (*m/z*) 568 ([M + H]⁺).

N-(Amino(3,5-dichloro-4-(cyclopropanecarboxamido)benzylamino)methylene)-3-(4-methoxyphenyl)-5-methylisoxazole-4-carboxamide (**17n**). Compound **17n** was prepared from **14a** via method B using 3,5-dichloro-4-(cyclopropanecarboxamido)benzylamine as amine **15**. Preparative HPLC purification afforded 23.6 mg (37% yield from **14a**) of **17n** as a white solid. ¹H NMR (500 MHz, CD₃OD) δ 7.61 (d, *J* = 8.9 Hz, 2H), 7.46 (br s, 2H), 7.04 (d, *J* = 8.9 Hz, 2H), 4.57 (br s, 2H), 3.84 (s, 3H), 2.67 (s, 3H), 1.93–1.83 (m, 1H), 1.01–0.86 (m, 4H). MS (ESI+) (*m/z*) 516 ([M + H]⁺).

N-(Amino(3-chloro-4-(cyclopropanecarboxamido)-5-methylbenzylamino)methylene)-3-(4-methoxyphenyl)-5-methylisoxazole-4-carboxamide (**17o**). Compound **17o** was prepared from **14a** via method B using 3-chloro-4-(cyclopropanecarboxamido)-5-methylbenzylamine as amine **15**. Preparative HPLC purification afforded 23.7 mg (97% yield from **14a**) of **17o** as a white solid. ¹H NMR (400 MHz, CD₃OD) δ 7.61 (d, *J* = 9.0 Hz, 2H), 7.32 (br s, 1H), 7.19 (br s, 1H), 7.05 (d, *J* = 8.8 Hz, 2H), 4.53 (br s, 2H), 3.84 (s, 3H), 2.67 (s, 3H), 2.26 (s, 3H), 1.83–1.92 (m, 1H), 0.85–1.00 (m, 4H). MS (ESI+) (*m/z*) 496 ([M + H]⁺).

N-(Amino(3-chloro-4-(furan-2-carboxamido)-5-methylbenzylamino)methylene)-3-(4-methoxyphenyl)-5-methylisoxazole-4-carboxamide (**17p**). Compound **17p** was prepared from **14a** via method B using 3-chloro-4-(furan-2-carboxamido)-5-methylbenzylamine as amine **15**. Preparative HPLC purification afforded 14.4 mg (57% yield from **14a**) of **17p** as a white solid. ¹H NMR (400 MHz, CD₃OD) δ 7.76 (d, *J* = 1.0 Hz, 1H), 7.63 (d, *J* = 8.8 Hz, 2H), 7.38 (br s, 1H), 7.22–7.30 (m, 2H), 7.03–7.09 (m, 2H), 6.67 (dd, *J* = 3.5, 1.8 Hz, 1H), 4.56 (br s, 2H), 3.85 (s, 3H), 2.68 (s, 3H), 2.32 (s, 3H). MS (ESI+) (*m/z*) 522 ([M + H]⁺).

N-(Amino(3,5-dichloro-4-(2-(dimethylamino)acetamido)benzylamino)methylene)-3-(4-methoxyphenyl)-5-methylisoxazole-4-carboxamide (**17q**). *N*-((4-(2-Bromoacetamido)-3,5-dichlorobenzylamino)(*tert*-butoxycarbonylamino)methylene)-3-(4-methoxyphenyl)-5-methylisoxazole-4-carboxamide (22 mg, 0.033 mmol) was dissolved in 2 mL of anhydrous DCM, followed by the addition of dimethylamine (0.085 mL of 2.0 M solution in methanol, 0.17 mmol). The reaction mixture was stirred at room temperature overnight, and then the reaction mixture was concentrated in vacuo. To the residue was added 0.8 mL of 50% TFA in DCM, and the resulting solution was stirred at room temperature for 1 h and then concentrated in vacuo and purified by preparative HPLC (0.1% TFA, MeOH/water) to afford 9.8 mg (39% yield) of **17q** as a white solid. ¹H NMR (500 MHz, CD₃OD) δ 7.60 (d, *J* = 8.5 Hz, 2H), 7.52 (br s, 2H), 7.03 (d, *J* = 8.5 Hz, 2H), 4.60 (br s, 2H), 4.29 (s, 2H), 3.84 (s, 3H), 3.02 (s, 6H), 2.67 (s, 3H). MS (ESI+) (*m/z*) 533 ([M + H]⁺).

N-(Amino(3-chloro-4-(2-(dimethylamino)acetamido)-5-methylbenzylamino)methylene)-3-(4-methoxyphenyl)-5-methylisoxazole-4-carboxamide (**17r**). Compound **17r** was prepared from **14a** via method B using 3-chloro-4-(2-(dimethylamino)acetamido)-5-methylbenzylamine as amine **15**. Preparative HPLC purification afforded 16.8 mg (67% yield from **14a**) of **17r** as a white solid. ¹H NMR (400 MHz, CD₃OD) δ 7.59 (d, *J* = 9.0 Hz, 2H), 7.38 (s, 1H), 7.26 (s, 1H), 7.02 (d, *J* = 8.8 Hz, 2H), 4.55 (s, 2H), 4.29 (s, 2H), 3.83 (s, 3H), 3.01 (s, 6H), 2.66 (s, 3H), 2.30 (s, 3H). MS (ESI+) (*m/z*) 513 ([M + H]⁺).

N-(Amino(3-chloro-5-(thiophen-3-yl)benzylamino)methylene)-3-(4-methoxyphenyl)-5-methylisoxazole-4-carboxamide (**19a**). Compound **8r** (19 mg, 40 μmol) was heated with 3-thiophenylboronic acid (15 mg), tetrakis(triphenylphosphine)palladium (5 mg), and aqueous tripotassium phosphate (2 M, 0.1 mL) in DMF (1.5 mL, degas with N₂) at 85 °C for 15 h. The crude mixture was purified by preparative HPLC to afford 7.5 mg of **19a** (30% yield from **8r**). ¹H NMR (500 MHz, CD₃OD) δ 7.75 (dd, *J*₁ = 1.46 Hz, *J*₂ = 2.93 Hz, 1H), 7.70 (dd, *J*₁ = 1.46 Hz, *J*₂ = 1.83 Hz, 1H), 7.62 (m, 3H), 7.53 (dd, *J*₁ = 2.93 Hz, *J*₂ = 5.12 Hz, 1H), 7.48 (dd, *J*₁ = 1.46 Hz, *J*₂ = 5.12 Hz, 1H), 7.31 (s, 1H), 7.02 (d, *J* = 8.8 Hz, 2H), 5.36 (d, *J* = 11 Hz, 1H), 4.61 (s, 2H), 3.82 (s, 3H), 2.67 (s, 3H). MS (ESI+) (*m/z*) 481 ([M + H]⁺).

N-(Amino(3-chloro-5-(pyridin-3-yl)benzylamino)methylene)-3-(4-methoxyphenyl)-5-methylisoxazole-4-carboxamide (**19b**). Compound **19b** was prepared by analogy to **19a**, substituting 3-pyridylboronic acid for 3-thiophenylboronic acid to afford 12.4 mg (42% yield from **8r**) of **19b** as a white solid. ¹H NMR (500 MHz, CD₃OD) δ 9.09 (s, 1H), 8.80 (d, *J* = 4.27 Hz, 1H), 8.65 (d, *J* = 8.24 Hz, 1H), 7.98 (dd, *J*₁ = 5 Hz, *J*₂ = 8.24 Hz, 1H), 7.84 (s, 1H), 7.71 (s, 1H), 7.58 (d, *J* = 8.8 Hz, 2H), 7.57 (s, 1H), 7.00 (d, *J* = 8.8 Hz, 2H), 5.36 (d, *J* = 11 Hz, 1H), 4.68 (s, 2H), 3.82 (s, 3H), 2.67 (s, 3H). MS (ESI+) (*m/z*) 476 ([M + H]⁺).

N-(Amino(3-chloro-5-(vinylbenzylamino)methylene)-3-(4-methoxyphenyl)-5-methylisoxazole-4-carboxamide (**19c**). Compound **19c** was prepared by analogy to **19a**, substituting 4,4,5,5-tetramethyl-2-vinyl-1,3,2-dioxaborolane for 3-thiophenylboronic acid to afford 7.5 mg (33% yield from **8r**) of **19c** as a white solid. ¹H NMR (500 MHz, CD₃OD) δ 7.61 (d, *J* = 8.8 Hz, 2H), 7.46 (s, 1H), 7.36 (s, 1H), 7.29 (s, 1H), 7.04 (d, *J* = 8.8 Hz, 2H), 6.73 (dd, *J*₁ = 17.4 Hz, *J*₂ = 11 Hz, 1H), 5.86 (d, *J* = 17.4 Hz, 1H), 5.36 (d, *J* = 11 Hz, 1H), 4.56 (s, 2H), 3.84 (s, 3H), 2.67 (s, 3H). MS (ESI+) (*m/z*) 425 ([M + H]⁺).

N-(Amino(3-chloro-5-((*E*)-4-hydroxybut-1-enyl)benzylamino)methylene)-3-(4-methoxyphenyl)-5-methylisoxazole-4-carboxamide (**19d**). Compound **19d** was prepared by analogy to **19a**, substituting (*E*)-trimethyl((4-(4,4,5,5-tetramethyl-1,3,2-dioxaborolan-2-yl)but-3-en-1-yl)oxy)silane for 3-thiophenylboronic acid to afford 2 mg (8% yield from **8r**) of **19d** as a white solid. MS (ESI+) (*m/z*) 469 ([M + H]⁺).

N-(Amino(3-chloro-5-((*E*)-pent-1-enyl)benzylamino)methylene)-3-(4-methoxyphenyl)-5-methylisoxazole-4-carboxamide (**19e**). Compound **19e** was prepared by analogy to **19a**, substituting (*E*)-4,4,5,5-tetramethyl-2-(pent-1-en-1-yl)-1,3,2-dioxaborolane for 3-thiophenylboronic acid to afford 9 mg (37% yield from **8r**) of **19e** as a white solid. ¹H NMR (500 MHz, CD₃OD) δ 7.62 (d, *J* = 8.24 Hz, 2H), 7.38 (s, 1H), 7.29 (s, 1H), 7.21 (s, 1H), 7.04 (d, *J* = 8.24 Hz, 2H), 6.39 (s, 2H), 4.54 (s, 2H), 3.84 (s, 3H), 2.67 (s, 3H), 2.22 (m, 2H), 1.51 (m, 2H), 0.97 (t, *J* = 7.32 Hz, 3H). MS (ESI+) (*m/z*) 467 ([M + H]⁺).

N-(Amino(3-chloro-5-((*E*)-3-methoxyprop-1-enyl)benzylamino)methylene)-3-(4-methoxyphenyl)-5-methylisoxazole-4-carboxamide (**19f**). Compound **19f** was prepared by analogy to **19a**, substituting (*E*)-2-(3-methoxyprop-1-en-1-yl)-4,4,5,5-tetramethyl-1,3,2-dioxaborolane for 3-thiophenylboronic acid to afford 8.1 mg (33% yield from **8r**) of **19f** as a white solid. ¹H NMR (500 MHz, CD₃OD) δ 7.62 (d, *J* = 8.5 Hz, 2H), 7.45 (s, 1H), 7.36 (s, 1H), 7.28 (s, 1H), 7.04 (d, *J* = 8.5 Hz, 2H), 6.64 (d, *J* = 14.7, 1H), 6.43 (m, 1H), 4.56 (s, 2H), 4.10 (d, *J* = 5.8 Hz, 2H), 3.85 (s, 3H), 3.39 (s, 3H), 2.68 (s, 3H). MS (ESI+) (*m/z*) 469 ([M + H]⁺).

N-((4-(2-Bromoacetamido)-3,5-dichlorobenzylamino)(*tert*-butoxycarbonylamino)methylene)-3-(4-methoxyphenyl)-5-methylisothiazole-4-carboxamide (**20a**). Intermediate **16a** (1.00 g, 1.77

mmol) was dissolved in 20 mL of anhydrous DCM in a 100 mL round-bottom flask, followed by the addition of 0.272 mL (1.95 mmol, 1.1 equiv) of triethylamine. The solution was cooled to 0 °C, and nitrogen was introduced. Bromoacetyl bromide (0.170 mL, 1.95 mmol, 1.1 equiv) was added dropwise, and the reaction mixture was stirred at 0 °C for 1 h. More bromoacetyl bromide (another 0.120 mL) was added and the reaction mixture was stirred at 0 °C for 1 h. DCM (80 mL) and saturated NaHCO₃ aqueous solution (100 mL) were added and the layers were separated. The aqueous was extracted with DCM (100 mL). The combined organic extracts were dried over anhydrous sodium sulfate. The crude product was purified by flash chromatography (EtOAc/DCM, 5:95) to give 1.18 g (98% yield) of **20a**. ¹H NMR (500 MHz, CDCl₃) δ 12.13 (s, 1H), 8.80 (br s, 1H), 7.96 (br s, 1H), 7.48 (d, J = 8.5 Hz, 2H), 7.12 (s, 2H), 6.86 (d, J = 8.9 Hz, 2H), 4.08 (s, 2H), 4.03 (d, J = 5.8 Hz, 2H), 3.80 (s, 3H), 2.68 (s, 3H), 1.53 (s, 9H). MS (ESI+) (*m/z*) 684 ([M + H]⁺).

N-(4-(2-Bromoacetamido)-3-chloro-5-methylbenzylamino)(tert-butoxycarbonylamino)methylene)-3-(4-methoxyphenyl)-5-methylisothiazole-4-carboxamide (**20b**). Compound **20b** (1.15 g) was prepared by analogy to compound **20a**, substituting **16b** for **16a** to afford 1.07 g (88% yield) of **20b** as a white solid. ¹H NMR (500 MHz, CDCl₃) δ 12.11 (s, 1H), 8.73 (s, 1H), 7.86 (s, 1H), 7.49 (d, J = 8.7, 2H), 7.05 (s, 1H), 6.91 (s, 1H), 6.87 (d, J = 8.7, 2H), 4.06 (s, 2H), 4.02 (d, J = 5.5 Hz, 2H), 3.77 (s, 3H), 2.67 (s, 3H), 2.24 (s, 3H), 1.50 (s, 9H). MS (ESI+) (*m/z*) 664 ([M + H]⁺).

N-(Amino(3,5-dichloro-4-(2-(dimethylamino)acetamido)-benzylamino)methylene)-3-(4-methoxyphenyl)-5-methylisothiazole-4-carboxamide (**22a**). Compound **20a** (26 mg, 0.038 mmol) was dissolved in 2 mL of anhydrous DCM, followed by the addition of dimethylamine (0.095 mL of 2.0 M methanol solution, 0.19 mmol) and DIPEA (25 mg, 0.19 mmol). The reaction mixture was stirred at room temperature overnight, and then the reaction mixture was concentrated in vacuo. To the residue was added 0.8 mL of 50% TFA in DCM, and the resulting solution was stirred at room temperature for 1 h, then concentrated in vacuo and purified by preparative HPLC (0.1% TFA, MeOH/water) to afford 14.5 mg (49% yield) of **22a** as a white solid. ¹H NMR (500 MHz, CD₃OD) δ 7.59 (d, J = 8.9 Hz, 2H), 7.49 (br s, 2H), 7.01 (d, J = 8.5 Hz, 2H), 4.60

N-(Amino(3-chloro-4-(2-(dimethylamino)acetamido)-5-methylbenzylamino)methylene)-3-(4-methoxyphenyl)-5-methylisothiazole-4-carboxamide (**22b**). Compound **22b** was prepared by analogy to **22a**, substituting **20b** for **20a**. Preparative HPLC purification afforded 47 mg (48% yield from **20b**) of **22b** as a white powder. ¹H NMR (500 MHz, CD₃OD) δ 7.59 (d, J = 8.9 Hz, 2H), 7.35 (br s, 1H), 7.23 (br s, 1H), 7.00 (d, J = 8.9 Hz, 2H), 4.56 (br s, 2H), 4.28 (s, 2H), 3.82 (br s, 3H), 3.02 (s, 6H), 2.71 (s, 3H), 2.31 (s, 3H). MS (ESI+) (*m/z*) 529 ([M + H]⁺).

N-(Amino(4-(2-(benzylamino)acetamido)-3,5-dichlorobenzylamino)methylene)-3-(4-methoxyphenyl)-5-methylisothiazole-4-carboxamide (**22c**). Compound **22c** was prepared by analogy to **22a**, substituting benzylamine for dimethylamine. Preparative HPLC purification afforded 24.7 mg (72% yield from **20a**) of **22c** as a white solid. ¹H NMR (500 MHz, CD₃OD) δ 7.58 (d, J = 8.9 Hz, 2H), 7.44–7.55 (m, 7H), 7.00 (d, J = 8.9 Hz, 2H), 4.60 (br s, 2H), 4.32 (s, 2H), 4.11 (s, 2H), 3.82 (s, 3H), 2.72 (s, 3H). MS (ESI+) (*m/z*) 611 ([M + H]⁺).

N-(Amino(4-(2-(benzylamino)acetamido)-3-chloro-5-methylbenzylamino)methylene)-3-(4-methoxyphenyl)-5-methylisothiazole-4-carboxamide (**22d**). Compound **22d** was prepared by analogy to **22a**, substituting **20b** for **20a**. Preparative HPLC purification afforded 22.0 mg (71% yield from **20b**) of **22d** as a white solid. ¹H NMR (500 MHz, CD₃OD) δ 7.58 (d, J = 8.5 Hz, 2H), 7.46–7.55 (m, 5H), 7.34 (br s, 1H), 7.22 (br s, 1H), 7.00 (d, J = 8.9 Hz, 2H), 4.55 (br s, 2H), 4.32 (s, 2H), 4.10 (s, 2H), 3.82 (s, 3H), 2.71 (s, 3H), 2.29 (s, 3H). MS (ESI+) (*m/z*) 591 ([M + H]⁺).

N-(Amino(3,5-dichloro-4-(2-(ethylamino)acetamido)-benzylamino)methylene)-3-(4-methoxyphenyl)-5-methylisothiazole-4-carboxamide (**22e**). Compound **22e** was prepared by analogy to **22a**, substituting ethylamine for dimethylamine. Preparative HPLC purification afforded 19.1 mg (68% yield from **20a**) of **22e** as a white solid. ¹H NMR (500 MHz, CD₃OD) δ 7.59 (d, J = 8.5 Hz, 2H), 7.48

(br s, 2H), 7.00 (d, J = 8.9 Hz, 2H), 4.60 (br s, 2H), 4.12 (s, 2H), 3.82 (s, 3H), 3.18 (q, J = 7.3 Hz, 2H), 2.72 (s, 3H), 1.35 (t, J = 7.3 Hz, 3H). MS (ESI+) (*m/z*) 549 ([M + H]⁺).

N-(Amino(3-chloro-4-(2-(ethylamino)acetamido)-5-methylbenzylamino)methylene)-3-(4-methoxyphenyl)-5-methylisothiazole-4-carboxamide (**22f**). Compound **22f** was prepared by analogy to **22a**, substituting **20b** for **20a**. Preparative HPLC purification afforded 18.7 mg (65% yield from **20b**) of **22d** as a white solid. ¹H NMR (500 MHz, CD₃OD) δ 7.58 (d, J = 8.9 Hz, 2H), 7.34 (br s, 1H), 7.22 (br s, 1H), 7.00 (d, J = 8.9 Hz, 2H), 4.55 (br s, 2H), 4.11 (s, 2H), 3.82 (s, 3H), 3.17 (q, J = 7.3 Hz, 2H), 2.71 (s, 3H), 2.31 (s, 3H), 1.36 (t, J = 7.3 Hz, 3H). MS (ESI+) (*m/z*) 529 ([M + H]⁺).

N-(Amino(4-(2-(azetidin-1-yl)acetamido)-3,5-dichlorobenzylamino)methylene)-3-(4-methoxyphenyl)-5-methylisothiazole-4-carboxamide (**22g**). Compound **22g** was prepared by analogy to **22a**, substituting azetidine for dimethylamine. Preparative HPLC purification afforded 6.4 mg (21% yield from **20a**) of **22g** as a white solid. ¹H NMR (500 MHz, CD₃OD) δ 7.59 (d, J = 8.9 Hz, 2H), 7.47 (br s, 2H), 7.01 (d, J = 8.9 Hz, 2H), 4.59 (br s, 2H), 4.40 (s, 2H), 4.34 (br s, 2H), 4.19 (br s, 2H), 3.82 (s, 3H), 2.72 (s, 3H). MS (ESI+) (*m/z*) 561 ([M + H]⁺).

N-(Amino(4-(2-(azetidin-1-yl)acetamido)-3-chloro-5-methylbenzylamino)methylene)-3-(4-methoxyphenyl)-5-methylisothiazole-4-carboxamide (**22h**). Step 1. Compound **20b** (100 mg) was added to 1.0 mL of 50% TFA in DCM. The resulting solution was stirred at room temperature for 1 h. DCM and TFA were evaporated in vacuo to give (E)-*N*-(amino(4-(2-bromoacetamido)-3-chloro-5-methylbenzylamino)methylene)-3-(4-methoxyphenyl)-5-methylisothiazole-4-carboxamide as a TFA salt, which was used without further purification. ¹H NMR (500 MHz, CD₃OD) δ 7.58 (d, J = 8.6, 2H), 7.29 (s, 1H), 7.17 (s, 1H), 6.99 (d, J = 8.6, 2H), 4.52 (s, 2H), 4.04 (s, 2H), 3.81 (s, 3H), 2.70 (s, 3H), 2.28 (s, 3H). MS (ESI+) (*m/z*) 564 ([M + H]⁺).

Step 2. To the crude product from Step 1 was added 4 mL of anhydrous DCM, followed by the addition of azetidine (25 mg, 0.44 mmol). The resulting reaction mixture was stirred at room temperature overnight. The residual solvent was evaporated in vacuo to give a crude product, which was purified by preparative HPLC to yield 80.9 mg (72% from **20b**) of **22h**. ¹H NMR (500 MHz, CDCl₃) δ 8.79 (br s, 1H), 7.54 (d, J = 7.3 Hz, 2H), 6.97 (br s, 1H), 6.86 (d, J = 7.3 Hz, 2H), 6.82 (br s, 1H), 3.96 (br s, 2H), 3.80 (s, 3H), 3.48 (t, J = 7.0 Hz, 4H), 3.29 (s, 2H), 2.56 (s, 3H), 2.13–2.24 (m, 5H). HRMS (ESI+): calculated for C₂₆H₃₀N₆O₃ClS, [M + H]⁺ = 541.1783; observed, [M + H]⁺ = 541.1769.

X-ray Crystallography. As previously reported,¹³ co-crystals of BACE-1 were prepared using a Phe-statine peptide and used in the following soaking experiments.

Compound 8k. The crystals were soaked with 2.5 mM **8k**, 35% PEG8K, 0.2 M ammonium sulfate, and 0.1 M sodium cacodylate at pH 6.2 for nine days. The resulting X-ray diffraction data indicated partial displacement of the Phe-statine peptide, and only the 3,5-dichlorobenzyl group of **8k** could be observed.

Compound 17d. The crystals were soaked with 10 mM **17d**, 18% PEGSK MME, 0.2 M ammonium iodide, and 0.1 M sodium citrate at pH 6.4 for 10 days. The resulting X-ray diffraction data indicated complete displacement of the Phe-statine peptide, and the X-ray structure was solved with a resolution of 2.65 Å. The coordinates for the complex of **17d** with BACE-1 have been deposited in the Protein Data Bank (www.pdb.org) under the PDB code 4SFE.

Compound 17g. The crystals were soaked with 10 mM **17g**, 18% PEGSK MME, 0.2 M ammonium iodide, and 0.1 M sodium citrate at pH 6.4 for 11 days. The resulting X-ray diffraction data indicated complete displacement of the Phe-statine peptide, and the X-ray structure was solved with a resolution of 2.5 Å. The coordinates for the complex of **17g** with BACE-1 have been deposited in the Protein Data Bank (www.pdb.org) under the PDB code 4FSL.

Biological Assays. Radioligand binding assays were conducted as described in ref 7. HEK-Sw and KBV-Sw cellular assays were conducted as described in ref 18.

Rat Studies. Rat studies were performed as described in refs 13 and 18.

■ ASSOCIATED CONTENT

Supporting Information

Additional SAR tables and experimental procedures for noncommercial benzylamines and compounds in the tables. This material is available free of charge via the Internet at <http://pubs.acs.org>.

Accession Codes

X-ray structures of **17d** (4SFE) and **17g** (4FSL) bound to BACE-1 have been deposited in the PDB (www.pdb.org).

■ AUTHOR INFORMATION

Corresponding Author

*Phone: 203-677-6884. Fax: 203-677-7884. Email: samuel.gerritz@bms.com.

Notes

The authors declare no competing financial interest.

■ ACKNOWLEDGMENTS

We acknowledge Hong Huang and Ivar MacDonald for their synthetic contributions, the Bioanalytical Research Group for the analysis of plasma, brain, and CSF drug levels, Rushith Anumula at Biocon Bristol-Myers Squibb R&D Center (Bangalore, India) for X-ray crystal structure refinements, Dieter Drexler for performing HRMS analyses, and Ramkumar Rajamani, Ken Boy, and Larry Marcin for helpful discussions.

■ ABBREVIATIONS USED

ABT, aminobenzotriazole; CYP P450, cytochrome P450; DIEA, diisopropylethylamine; DCM, dichloromethane; DIEA, diisopropylethylamine; DMAP, 4-*N,N*-dimethylaminopyridine; DMF, *N,N*-dimethyl formamide; EDC, 1-(3-dimethylamino-propyl)-3-ethylcarbodiimide hydrochloride; EtOH, ethanol; HOBT, 1-hydroxybenzotriazole; MeOH, methanol; NMP, *N*-methylpyrrolidinone; PyAOP, (7-azabenzotriazol-1-yloxy)-tripyrrolidinophosphonium hexafluorophosphate; PS, polystyrene; TFA, trifluoroacetic acid; THF, tetrahydrofuran

■ REFERENCES

- Querfurth, H. W.; LaFerla, F. M. Alzheimer's disease. *N. Engl. J. Med.* **2010**, *362*, 329–344.
- World Alzheimer Report 2011; Alzheimer's Disease International; <http://www.alz.co.uk> (accessed June 28, 2012).
- Walsh, D. M.; Selkoe, D. J. Ab oligomers—a decade of discovery. *J. Neurochem.* **2007**, *101*, 1172–1184.
- Citron, M. Alzheimer's disease: strategies for disease modification. *Nature Rev. Drug Discovery* **2010**, *9*, 387–398.
- McConlogue, L.; Buttini, M.; Anderson, J. P.; Brigham, E. F.; Chen, K. S.; Freedman, S. B.; Games, D.; Johnson-Wood, K.; Lee, M.; Zeller, M.; Liu, W.; Motter, R.; Sinha, S. Partial reduction of BACE1 has dramatic effects on Alzheimer plaque and synaptic pathology in APP Transgenic Mice. *J. Biol. Chem.* **2007**, *282*, 26326–26334.
- Ghosh, A. K.; Shin, D.; Downs, D.; Koelsch, G.; Lin, X.; Ermolieff, J.; Tang, J. Design of Potent Inhibitors for Human Brain Memapsin 2 (beta-Secretase). *J. Am. Chem. Soc.* **2000**, *122*, 3522–3523.
- Iben, L. G.; Kopcho, L.; Marcinkeviciene, J.; Zheng, C.; Thompson, L. A.; Albright, C. F.; Toyn, J. H. [3H]BMS-599240—a novel tritiated ligand for the characterization of BACE1 inhibitors. *Eur. J. Pharmacol.* **2008**, *593*, 10–15.
- Kuntz, I. D.; Chen, K.; Sharp, K. A.; Kollman, P. A. The maximal affinity of ligands. *Proc. Natl. Acad. Sci. U. S. A.* **1999**, *96*, 9997–10002.

(9) Hopkins, A. L.; Groom, C. R.; Alex, A. Ligand efficiency: a useful metric for lead selection. *Drug Discovery Today* **2004**, *9*, 430–431.

(10) Dodd, D. S.; Zhao, Y. Solid-phase synthesis of *N,N'*-substituted acylguanidines. *Tetrahedron Lett.* **2001**, *42*, 1259–1262.

(11) Wang, S. S. *p*-Alkoxybenzyl alcohol resin and *p*-alkoxybenzyloxycarbonylhydrazide resin for solid phase synthesis of protected peptide fragments. *J. Am. Chem. Soc.* **1973**, *95*, 1328–1333.

(12) McGregor, D. N.; Corbin, U.; Swigor, J. E.; Cheney, L. C. Synthesis of isothiazoles: the transformation of isoxazoles into isothiazoles. *Tetrahedron* **1969**, *25*, 389–395.

(13) Thompson, L. A.; Shi, J.; Decicco, C. P.; Tebben, A. J.; Olson, R. E.; Boy, K. M.; Guernon, J. M.; Good, A. C.; Liauw, A.; Zheng, C.; Copeland, R. A.; Combs, A. P.; Trainor, G. L.; Camac, D. M.; Muckelbauer, J. K.; Lentz, K. A.; Grace, J. E.; Burton, C. R.; Toyn, J. H.; Barten, D. M.; Marcinkeviciene, J.; Meredith, J. E.; Albright, C. F.; Macor, J. E. Synthesis and in vivo evaluation of cyclic diaminopropane BACE-1 inhibitors. *Bioorg. Med. Chem. Lett.* **2011**, *21*, 6909–6915.

(14) Marcin, L. R.; Higgins, M. A.; Zusi, F. C.; Zhang, Y.; Dee, M. F.; Parker, M. F.; Muckelbauer, J. K.; Camac, D. M.; Morin, P. E.; Ramamurthy, V.; Tebben, A. J.; Lentz, K. A.; Grace, J. E.; Marcinkeviciene, J. A.; Kopcho, L. M.; Burton, C. R.; Barten, D. M.; Toyn, J. H.; Meredith, J. E.; Albright, C. F.; Bronson, J. J.; Macor, J. E.; Thompson, L. A. Synthesis and SAR of indole- and 7-azaindole-1,3-dicarboxamide hydroxyethylamine inhibitors of BACE-1. *Bioorg. Med. Chem. Lett.* **2011**, *21*, 537–541.

(15) Stachel, S. J.; Coburn, C. A.; Steele, T. G.; Crouthamel, M. C.; Pietrak, B. L.; Lai, M. T.; Holloway, M. K.; Munshi, S. K.; Graham, S. L.; Vacca, J. P. Conformationally biased P3 amide replacements of beta-secretase inhibitors. *Bioorg. Med. Chem. Lett.* **2006**, *16*, 641–644.

(16) *The PyMOL Molecular Graphics System*, version 1.3r1; Schrodinger LLC, 2010.

(17) Chenguang, Y.; Williams, R. M. An efficient method for the preparation of amidinouras. *Tetrahedron Lett.* **1996**, *37*, 1945–1948.

(18) Meredith, J. E., Jr.; Thompson, L. A.; Toyn, J. H.; Marcin, L.; Barten, D. M.; Marcinkeviciene, J.; Kopcho, L.; Kim, Y.; Lin, A.; Guss, V.; Burton, C.; Iben, L.; Polson, C.; Cantone, J.; Ford, M.; Drexler, D.; Fiedler, T.; Lentz, K. A.; Grace, J. E., Jr.; Kolb, J.; Corsa, J.; Pierdomenico, M.; Jones, K.; Olson, R. E.; Macor, J. E.; Albright, C. F. P-glycoprotein efflux and other factors limit brain amyloid beta reduction by beta-site amyloid precursor protein-cleaving enzyme 1 inhibitors in mice. *J. Pharmacol. Exp. Ther.* **2008**, *326*, 502–513.

(19) Stachel, S. J.; Coburn, C. A.; Rush, D.; Jones, K. L.; Zhu, H.; Rajapakse, H.; Graham, S. L.; Simon, A.; Katharine Holloway, M.; Allison, T. J.; Munshi, S. K.; Espeseth, A. S.; Zuck, P.; Colussi, D.; Wolfe, A.; Pietrak, B. L.; Lai, M. T.; Vacca, J. P. Discovery of aminoheterocycles as a novel beta-secretase inhibitor class: pH dependence on binding activity part 1. *Bioorg. Med. Chem. Lett.* **2009**, *19*, 2977–2980.

(20) Stachel, S. J.; Steele, T. G.; Petrocchi, A.; Haugabook, S. J.; McGaughey, G.; Katharine Holloway, M.; Allison, T.; Munshi, S.; Zuck, P.; Colussi, D.; Tugasheva, K.; Wolfe, A.; Graham, S. L.; Vacca, J. P. Discovery of pyrrolidine-based beta-secretase inhibitors: lead advancement through conformational design for maintenance of ligand binding efficiency. *Bioorg. Med. Chem. Lett.* **2012**, *22*, 240–244.

(21) Weaver, C. D.; Harden, D.; Dworetzky, S. I.; Robertson, B.; Knox, R. J. A thallium-sensitive, fluorescence-based assay for detecting and characterizing potassium channel modulators in mammalian cells. *J. Biomol. Screening* **2004**, *9*, 671–677.

(22) Fox, E.; Bates, S. E. Tariquidar (XR9576): a P-glycoprotein drug efflux pump inhibitor. *Expert Rev. Anticancer Ther.* **2007**, *7*, 447–459.

(23) Cole, D. C.; Bursavich, M. G. Nonpeptide BACE1 Inhibitors: Design and Synthesis. In *Aspartic Acid Proteases as Therapeutic Targets*; Wiley-VCH Verlag GmbH & Co. KGaA: New York, 2010; pp 481–509.

(24) Zhu, Z.; Sun, Z. Y.; Ye, Y.; Voigt, J.; Strickland, C.; Smith, E. M.; Cumming, J.; Wang, L.; Wong, J.; Wang, Y. S.; Wyss, D. F.; Chen, X.; Kuvellkar, R.; Kennedy, M. E.; Favreau, L.; Parker, E.; McKittrick, B. A.; Stamford, A.; Czarniecki, M.; Greenlee, W.; Hunter, J. C. Discovery of cyclic acylguanidines as highly potent and selective beta-site amyloid

cleaving enzyme (BACE) inhibitors: Part I—inhibitor design and validation. *J. Med. Chem.* **2010**, *53*, 951–965.

(25) Cole, D. C.; Manas, E. S.; Stock, J. R.; Condon, J. S.; Jennings, L. D.; Aulabaugh, A.; Chopra, R.; Cowling, R.; Ellingboe, J. W.; Fan, K. Y.; Harrison, B. L.; Hu, Y.; Jacobsen, S.; Jin, G.; Lin, L.; Lovering, F. E.; Malamas, M. S.; Stahl, M. L.; Strand, J.; Sukhdeo, M. N.; Svenson, K.; Turner, M. J.; Wagner, E.; Wu, J.; Zhou, P.; Bard, J. Acylguanidines as small-molecule beta-secretase inhibitors. *J. Med. Chem.* **2006**, *49*, 6158–6161.

(26) Fobare, W. F.; Solvibile, W. R.; Robichaud, A. J.; Malamas, M. S.; Manas, E.; Turner, J.; Hu, Y.; Wagner, E.; Chopra, R.; Cowling, R.; Jin, G.; Bard, J. Thiophene substituted acylguanidines as BACE1 inhibitors. *Bioorg. Med. Chem. Lett.* **2007**, *17*, 5353–5356.

(27) Cole, D. C.; Stock, J. R.; Chopra, R.; Cowling, R.; Ellingboe, J. W.; Fan, K. Y.; Harrison, B. L.; Hu, Y.; Jacobsen, S.; Jennings, L. D.; Jin, G.; Lohse, P. A.; Malamas, M. S.; Manas, E. S.; Moore, W. J.; O'Donnell, M. M.; Olland, A. M.; Robichaud, A. J.; Svenson, K.; Wu, J.; Wagner, E.; Bard, J. Acylguanidine inhibitors of beta-secretase: optimization of the pyrrole ring substituents extending into the S1 and S3 substrate binding pockets. *Bioorg. Med. Chem. Lett.* **2008**, *18*, 1063–1066.

(28) Malamas, M. S.; Barnes, K.; Johnson, M.; Hui, Y.; Zhou, P.; Turner, J.; Hu, Y.; Wagner, E.; Fan, K.; Chopra, R.; Olland, A.; Bard, J.; Pangalos, M.; Reinhart, P.; Robichaud, A. J. Di-substituted pyridinyl aminohydantoin as potent and highly selective human beta-secretase (BACE1) inhibitors. *Bioorg. Med. Chem.* **2010**, *18*, 630–639.

(29) Malamas, M. S.; Erdei, J.; Gunawan, I.; Turner, J.; Hu, Y.; Wagner, E.; Fan, K.; Chopra, R.; Olland, A.; Bard, J.; Jacobsen, S.; Magolda, R. L.; Pangalos, M.; Robichaud, A. J. Design and synthesis of 5,5'-disubstituted aminohydantoin as potent and selective human beta-secretase (BACE1) inhibitors. *J. Med. Chem.* **2010**, *53*, 1146–1158.

(30) Malamas, M. S.; Erdei, J.; Gunawan, I.; Barnes, K.; Johnson, M.; Hui, Y.; Turner, J.; Hu, Y.; Wagner, E.; Fan, K.; Olland, A.; Bard, J.; Robichaud, A. J. Aminoimidazoles as potent and selective human beta-secretase (BACE1) inhibitors. *J. Med. Chem.* **2009**, *52*, 6314–6323.

(31) Baxter, E. W.; Conway, K. A.; Kennis, L.; Bischoff, F.; Mercken, M. H.; Winter, H. L.; Reynolds, C. H.; Tounge, B. A.; Luo, C.; Scott, M. K.; Huang, Y.; Braeken, M.; Pieters, S. M.; Berthelot, D. J.; Masure, S.; Bruinzeel, W. D.; Jordan, A. D.; Parker, M. H.; Boyd, R. E.; Qu, J.; Alexander, R. S.; Breneman, D. E.; Reitz, A. B. 2-Amino-3,4-dihydroquinazolines as inhibitors of BACE-1 (beta-site APP cleaving enzyme): Use of structure based design to convert a micromolar hit into a nanomolar lead. *J. Med. Chem.* **2007**, *50*, 4261–4264.

(32) Barrow, J. C.; Stauffer, S. R.; Rittle, K. E.; Ngo, P. L.; Yang, Z.; Selnick, H. G.; Graham, S. L.; Munshi, S.; McGaughey, G. B.; Holloway, M. K.; Simon, A. J.; Price, E. A.; Sankaranarayanan, S.; Colussi, D.; Tugusheva, K.; Lai, M. T.; Espeseth, A. S.; Xu, M.; Huang, Q.; Wolfe, A.; Pietrak, B.; Zuck, P.; Levorse, D. A.; Hazuda, D.; Vacca, J. P. Discovery and X-ray crystallographic analysis of a spiropiperidine iminohydantoin inhibitor of beta-secretase. *J. Med. Chem.* **2008**, *51*, 6259–6262.